JNCI 17-1208R1

Article

Immune infiltration in invasive lobular breast cancer

Christine Desmedt[1], Roberto Salgado[1,2], Marco Fornili[3], Giancarlo Pruneri[4], Gert Van den Eynden[5], Gabriele Zoppoli[6], Françoise Rothé[1], Laurence Buisseret[1], Soizic Garaud[5], Karen Willard-Gallo[5], David Brown[1], Yacine Bareche[1], Ghizlane Rouas[1], Christine Galant[7], François Bertucci[8], Sherene Loi[9], Giuseppe Viale[4], Angelo Di Leo[10], Andrew R. Green[11], Ian O. Ellis[11,12], Emad A. Rakha[11,12], Denis Larsimont[13], Elia Biganzoli[3,*], Christos Sotiriou[1,*]

1. J.C. Heuson Breast Cancer Translational Research Laboratory, Université Libre de Bruxelles, Institut Jules Bordet, 1000 Brussels, Belgium

2. Department of Pathology, GZA Ziekenhuizen- Campus Sint Augustinus, Wilrijk, Belgium

3. Unit of Medical Statistics, Biometry and Bioinformatics "Giulio A. Maccacaro", Department of Clinical Sciences and Community Health, University of Milan Campus Cascina Rosa, Fondazione IRCCS Istituto Nazionale Tumori, Milan, Italy

4. Department of Pathology, European Institute of Oncology, University of Milan, Milan, Italy

5. Molecular Immunology Unit, Institut Jules Bordet, Université Libre de Bruxelles, Brussels, Belgium

6. Department of Internal Medicine (DiMI), University of Genoa and IRCCS San Martino-National Cancer Institute, Genoa, Italy

7. Department of Pathology, Cliniques Universitaires Saint Luc, Brussels, Belgium

8. Department of Medical Oncology, Institut Paoli-Calmettes, Marseille, France

9. Division of Research and Clinical Medicine, Peter MacCallum Cancer Centre, Melbourne, Victoria, Australia

10. Sandro Pitigliani Medical Oncology Unit, Hospital of Prato, Instituto Toscano Tumori,

59100 Prato, Italy

11. Academic Pathology, Division of Cancer and Stem Cells, School of Medicine, University of Nottingham, Nottingham City Hospital, Hucknall Road, Nottingham NG5 1PB

12. Histopathology, Nottingham University Hospitals NHS Trust, Hucknall Road, Nottingham, NG5 1PB

13. Department of Pathology, Institut Jules Bordet, Université Libre de Bruxelles, Brussels, Belgium

*These authors contributed equally to the present work.

Corresponding author:

Christine Desmedt

Breast Cancer Translational Research Laboratory (BCTL),

Institut Jules Bordet

125 Boulevard de Waterloo

1000 Brussels, Belgium

Phone: +32 541 34 28

Email: christine.desmedt@bordet.be

Word count: 3,130

Abstract

Background

Invasive lobular breast cancer (ILC) is the second most common histological subtype of breast cancer after invasive ductal cancer (IDC). Here, we aimed at evaluating the prevalence, levels and composition of tumor infiltrating lymphocytes (TIL) and their association with clinico-pathological, and outcome variables in ILC, and to compare it with IDC.

Methods

We considered two patient series with TIL data: a multi-centric retrospective series (n=614) and the BIG 02-98 study (n=149 ILC and 807 IDC). We compared immune subsets identified by immuno-histochemistry in the ILC (n=159) and IDC (n=468) patients from the Nottingham series, as well as the CIBERSORT immune profiling of the ILC (n=98) and IDC (n=388) METABRIC and TCGA patients. All ILC/IDC comparisons were done in ER-positive/HER2-negative tumors. All statistical tests were two-sided.

Results

TIL levels were statistically significantly lower in ILC compared to IDC (fold change =0.79; 95%CI: 0.70-0.88, $P<.001$). In ILC, high TIL levels were associated with young age, lymph node involvement, and high proliferative tumors. In the univariable analysis, high TIL levels were associated with worse prognosis in the retrospective and BIG 02-98 lobular series, although it did not reach statistical significance in the latter. The Nottingham series revealed that the levels of intra-tumoral but not total $CD8^+$ were statistically significantly lower in ILC compared to IDC. Comparison of the CIBERSORT profiles highlighted statistically significant differences in terms of immune composition.

Conclusion

This study shows differences between the immune infiltrates of ER-positive/HER2-negative ILC and IDC in terms of prevalence, levels, localization, composition, and clinical associations.

Introduction

The presence and potential clinical value of tumor infiltrating lymphocytes (TIL) has been assessed in many studies. Increased lymphocytic infiltration has been shown to be more frequent in triple negative and HER2-positive breast cancer and to be associated with an increased pathological complete response rate after neo-adjuvant, as well as with improved survival after adjuvant chemotherapy in these subtypes (1–3). Given that various methods have been used to quantify TIL in breast cancer, efforts to standardize its assessment were undertaken resulting in the first guidelines for scoring TIL (4). A recent publication also showed that the assessment of stromal TIL, those present in the tumor stromal tissue, is more reproducible than intratumoral TIL evaluation (5). A complementary approach to evaluate immune infiltrates is to apply a deconvolution algorithm to gene expression data, such as CIBERSORT which estimates the relative proportion of various immune cell types (6–8).

Invasive lobular breast cancer (ILC) represents the second most common histological subtype in breast cancer after invasive breast carcinoma of no special type (NST), previously known and further referred to as invasive ductal carcinoma (IDC), and accounts for up to 15% of cases (9). These tumors generally express ER and lack *HER2* amplification. Clinically, patients with ILC differ from those with IDC. They tend to relapse later and present a different metastatic pattern (9,10). Recently, The Cancer Genome Atlas (TCGA), the RATHER consortium, METABRIC and our group characterized the genomic landscape of a large number of ILC tumors and consistently demonstrated that ILC presents differences regarding the frequency of alterations in several cancer genes compared to IDC (11–14). Of potential relevance, the TCGA and RATHER consortia also identified an 'immune-related' ILC transcriptomic subtype. However, when comparing these immune subtypes on the same datasets, it seems that they were not identifying the same tumors, suggesting that their definition should be further investigated (11,12).

Whilst TIL in breast cancer continue to attract considerable attention, to our knowledge, there are no previous reports interrogating TIL in large cohorts of ILC. Using our multi-centric retrospective cohort of ILC (13), we aimed to evaluate the distribution of TIL, correlate TIL levels with standard

clinico-pathological parameters, investigate their prognostic value, and explore associations between TIL and transcriptomic features and recurrent genomic alterations in ILC. We further aimed to compare TIL between ER-positive/HER2-negative ILC and IDC tumors in the BIG 02-98 study (15). Finally, going beyond TIL to further enhance our understanding of the immune infiltrates in ER-positive/HER2-negative ILC and IDC tumors, we compared the proportion and localization of several immune subsets in the Nottingham series (16–18) and the estimates of the proportion of the different immune cell types provided by CIBERSORT in the METABRIC and TCGA cohorts (7,11,19).

Material and methods

Patients and samples

The retrospective multi-centric series of primary ILC has already been described[13]. **Supplementary Tables 1 and 2** provide overview and patient-level information, respectively, of the main clinical characteristics whilst **Supplementary Figure 1** reports the number of patients and samples considered for each analysis. The comparison of TIL in terms of prevalence and clinico-pathological associations between ER-positive/HER2-negative ILC (n=149) and IDC (n=807) was assessed in the BIG 02-98 study (**Supplementary Table 3**)(15). From this study we only considered those patients whose tumor samples underwent central revision for ER and HER2 (20). For the Nottingham series, we only considered the ER-positive/HER2-negative ILC (n=159) and IDC (n=468) cases (16–18). The patient and tumor characteristics from all investigated ER-positive/HER2-negative ILC and IDC cases are reported in **Supplementary Table 4**. This project has been approved by the ethics committee of the Institut Jules Bordet (CE1726 and CE2560).

Assessment of immune infiltration

Stromal TIL, which is the percentage of tumor stromal area containing TIL and hereinafter further referred to as TIL, were independently evaluated by three pathologists (GVE, GP and RS) on

hematoxylin and eosin-stained slides of the retrospective ILC cohort (n=614), using the protocols described in Salgado *et al*.(4). To evaluate the reliability of TIL assessments, the two-way random intra-class correlation coefficient (ICC) was estimated (21). All cases for which the discordance between at least two pathologists reached >15% were first independently re-scored by all three pathologists and then reviewed together until a consensus was reached. For each pathologist, consensus values were used to recalibrate the other measurements through Passing-Bablok regression (22). The log transformation was applied to TIL values in order to stabilize variance and achieve an approximately symmetric distribution according to the measurement process (23). In the analyses, the arithmetic mean over the three pathologists of the log values was used. In the BIG 02-98 study, TIL were assessed previously by two pathologists, including RS, using the same method and the results described in Loi *et al.*(15). For this study, we considered the arithmetic mean of the log values from the two pathologists.

Statistical Analysis

Univariable and multiple linear regression models of log-transformed TIL percentage versus clinico-pathological and genomic variables were fitted. Point estimates and 95% confidence intervals of fold change of TIL percentage were obtained. In the retrospective ILC cohort and the BIG2-98 series, we used the previously reported survival endpoints, namely breast cancer-free interval (BCFI) (13) and disease-free survival (DFS) (15), respectively. The association between the survival endpoints and the immune variables was evaluated using a Cox regression model by considering TIL as either continuous or categorical values and with or without adjustment for clinico-pathological variables. Statistical significance was assessed using the Wald test. For the comparison of the various immune markers in the Nottingham series, we recurred to the proportional odds logistic model extension of the Mann-Whitney test according to Harrell (24), to adjust for histology, age, grade, axillary lymph node status and Ki67. CIBERSORT data from the METABRIC and TCGA series were obtained from Ali *et al.*(7) (n= 98 ILC and n=388 IDC) and compared using Wilcoxon rank sum test. All statistical tests were two-sided and *P*-values <.05 were considered statistically significant. Whenever appropriate, we applied correction for

multiple testing using the Benjamini-Hochberg method ([25]). All analyses were performed using R v3.4.1 ([26]).

Results

Distribution of TIL

The intraclass correlation coefficient between the three pathologists for TIL evaluation on the 614 ILC cases from the multi-centric retrospective series was 0.71 (95%CI: 0.65-0.76). ILC was characterized by low lymphocytic infiltration, with a median percentage of TIL of 5% and an interquartile range of 3-7% (**Figure 1A**). Fifteen percent of the samples had more than 10% of TIL. We compared the distribution of TIL in ER-positive/HER2-negative ILC to ER-positive/HER2-negative IDC tumors from the BIG 02-98 study (15) and observed that TIL counts were slightly but statistically significantly lower in ILC compared to IDC (fold change = 0.79, 95%CI: 0.70-0.88, *P*<.001) (**Figure 1B**).

Association between TIL and clinico-pathological variables

We investigated the association between TIL as a continuous variable and the standard clinico-pathological variables. In the retrospective series, we observed at the univariable level, that higher TIL values were associated with ER and PR negative status, high proliferation status (≥20% Ki67), high grade, node positive status and young age at diagnosis (**Figure 2A**, **Supplementary Table 5**). We further observed a statistically significant increase and decrease of TIL for the mixed non-classic and the alveolar subtypes, respectively, compared to the more common classic subtype. In the multivariable regression, a similar trend was detected for these variables, with the exception of tumor grade for which the association was no longer statistically significant. The associations between TIL and age, as well as

Ki67 in all ILC patients from BIG 02-98 (n=204) were consistent with our results (**Supplementary Figure 2, Supplementary Table 6**). The association with lymph node involvement could not be investigated since all patients included in this trial had positive lymph nodes. When restricting the analyses to the ER-positive/HER2-positive ILC in our cohort (n=555), we made similar observations as in the global ILC population regarding the association with high Ki67, node positive status and young age at diagnosis (**Figure 2A**, **Supplementary Table 7**). We next used the TIL data collected in the BIG 02-98 trial to compare the associations in ER-positive/HER2-negative IDC (n=807) and ILC (n=149). TIL were positively associated with Ki67 both in IDC and ILC. However, the associations with age and with grade were restricted to ILC and IDC, respectively (**Figure 2B** and **Supplementary Tables 8-9**).

Association between TIL and genomic alterations

Genomic alterations with oncogenic potential (substitutions and indels as previously defined ([27])) were available for 399 patients of the multi-centric retrospective ILC series (13), leading us to evaluate the association between TIL and the mutational status of the 15 genes that were mutated in at least 2% of the tumors. We observed statistically significantly lower TIL counts in tumors harboring *ERBB3* mutations and higher TIL counts in tumors presenting somatic oncogenic *TP53*, *ARID1A* and *BRCA2* mutations compared with tumors that were not mutated in those genes. *KMT2C* and *PIK3CA* mutated tumors were associated with higher TIL, although not statistically significantly (**Figure 3A**, **Supplementary Table 10**). All associations remained statistically significant in multivariable models with standard clinico-pathological variables, with the exception of *BRCA2*. We further investigated the association between TIL and copy number aberrations (CNA) present in at least 5% of the patients. Genome-wide copy number data was available for 166 cases. We observed statistically significantly higher TIL values in tumors with 8q24.23 loss (which included *PTK2*) and 7p21.2 gains (*ETV1*), but statistically significantly lower TIL in tumors with 5q gains (**Figure 3B**, **Supplementary Table 11**).

Association between TIL and transcriptomic features

In order to better understand the transcriptomic phenotype associated with infiltrated ILC tumors, we compared the gene expression profiles between ILC tumors with low (≤5%) and high TIL levels (>10%), microarray gene expression data being available for 117 tumors of the multi-centric ILC cohort. Thirty-three genes were over-expressed in the high TIL-group with a fold change ≥1.2 compared to the low TIL-group, and a corrected $P \leq .05$. This list included, among others, genes involved in cellular defense response (GO:0006968; *ITK*, *CXCL9*, *TRAT1*, *SH2D1A* and *CCR6*) and regulation of antigen receptor-mediated signaling pathway (GO:0050854; *PRKCB*, *TRAT1*, *CCR7*, *UBASH3A*) (**Figure 3C**). We then computed a score based on these 33 genes and compared it with existing immune and other gene expression signature scores ([28–37]). We observed a strong correlation with several previously reported immune expression signatures (**Figure 3D**), suggesting that the immune infiltrates present in ILC might share at least some similarities with the ones found in the global breast cancer population.

Comparison of the prevalence and localization of different immune cell types between ER-positive/HER2-negative ILC and IDC

We further aimed at extending our immune comparison between ER-positive/HER2-negative ILC and IDC beyond TIL counts by interrogating immuno-histochemical data on various immune markers according to their localization (total staining or staining restricted to the intra-tumoral, adjacent or distant stromal compartments) in the Nottingham series (16–18), and the CIBERSORT immune profiles in the METABRIC and TCGA datasets(7).

We compared the scores for $CD3^+$, $CD8^+$, $CD20^+$, $CD68^+$ and $FOXP3^+$ cells between the 159 ILC and 468 IDC samples from the Nottingham series (**Figure 4A**). After adjusting for standard clinico-pathological variables, we observed statistically significantly lower levels in ILC compared to IDC regarding the adjacent stromal $CD3^+$, the intra-tumoral $CD8^+$, all measures of $CD68^+$, and all but not the intra-tumoral measures of $FOXP3^+$ cells. To complement this analysis, we compared the relative proportion of the various immune cell types recognized by CIBERSORT (7) and reported the statistically significant associations in **Supplementary Figure 4**. Importantly, as in Ali *et al.*(7), we considered only samples with a CIBERSORT p-value <0.05, excluding samples without immune

infiltration, leaving 388 ER-positive/HER2-negative IDC to the 98 ER-positive/HER2-negative ILC samples. The comparison revealed a lower frequency of follicular helper and gamma delta T cells, as well as M0, M1 and to a lesser extend M2 macrophages in ILC compared to IDC, but a higher frequency of B memory cells, monocytes and $CD8^+$ T cells. Unfortunately, these results do not provide information regarding the localization of these different immune cell types since CIBERSORT derives the immune subtyping from bulk transcriptomic data.

Association between TIL and survival

Finally, we assessed the prognostic value of TIL in ILC. TIL were initially considered as a continuous variable for survival analysis, revealing that higher TIL were associated with a worse prognosis in ILC in univariable (HR=1.22 for each 10% increment; 95%CI: 1.06-1.41, *P*=.005), but not multivariable analysis in the retrospective cohort (**Supplementary Table 12**). TIL were next considered as a categorical variable using the following groups, with the cutpoints adapted from the interquartile range rounded to the nearest multiple of 5: low (≤5%), intermediate (>5 and ≤10%) and high (>10%). Both the high and intermediate groups were associated with worse breast cancer free interval (BCFI) compared to the lowest TIL values ($HR_{high\ vs\ low}$= 1.84; 95%CI: 1.22-2.78, *P*=.004; $HR_{intermediate\ vs\ low}$= 1.46; 95%CI: 1.02-2.09, *P*=.04, **Figure 5A**). In multivariable analysis adjusting for the standard clinico-pathological variables, the association between BCFI and TIL in the group with high TIL values lost statistical significance whereas the association remained statistically significant for the group with intermediate TIL (**Supplementary Table 13**). Exploratory analyses in the ER-positive/HER2-negative subgroup revealed a biologically consistent but non-statistically significant difference between the high and low group (HR=1.58; 95CI: 0.98-2.54, *P*=.06, **Supplementary Table 14**), while no statistically significant difference was observed between the TIL groups in the ER-negative and/or HER2-positive subgroup (**Figure 5B**, **Supplementary Figure 3A**, **Supplementary Table 15**). We further assessed the prognostic value of TIL in the BIG 02-98 series and similarly to the retrospective cohort, we observed that higher TIL were associated with worse prognosis at the univariable level, although not reaching

statistical significance (**Figure 5C**, **Supplementary Table 16**). While the separation of the curves was visible for the ER-positive/HER2-negative ILC subgroup (**Figure 5D**, **Supplementary Table 17**), the curves were completely superimposed for the ER-positive/HER2-negative IDC (**Supplementary Figure 3B**, **Supplementary Table 18**).

Discussion

This work represents to our knowledge the most detailed and comprehensive assessment of TIL using standardized, reproducible protocols and the largest series of primary ILC samples to date. We demonstrated that most ILC are characterized by low levels of TIL. The vast majority of ILC tumors (~90%) are ER-positive/HER2-negative making our findings consistent with previous reports showing that TIL are more prevalent in triple-negative and HER2-positive breast cancer (15,38,39). Droeser *et al.* reported lower levels of lymphocytic infiltrates in ILC compared to IDC, based on the percentage of $CD4^+$ IHC-stained cells; however, this comparison was flawed since they included all IDC and ILC tumors irrespective of ER and HER2 status (40). Our comparison of ER-positive/HER2-negative ILC and IDC in the BIG 02-98 study however confirmed the slight but statistically significant increase in TIL in IDC, even after adjusting for clinico-pathological variables.

Several important findings emerged when comparing the associations between TIL, clinico-pathological variables, and survival between ER-positive/HER2-negative ILC and IDC. First, while high TIL levels were associated with high proliferation status as defined by Ki67 in both histological subtypes, the association of young age and high grade with high TIL levels was only seen in ILC and IDC, respectively. Second, the survival analyses in our retrospective ILC cohort revealed that increased TIL were associated with worse BCFI at the univariable level. This was the case when TIL were assessed either as a continuous or categorical variable. This observation was somehow contrasting to what has been reported in triple negative and HER2-positive breast cancer, where increased TIL were associated with better prognosis (1,2). However, in the multivariable analysis, TIL lost their prognostic value at the continuous level, although in the categorical analysis, the group with intermediate TIL values remained

associated with worse prognosis compared to the group with low TIL. This loss of prognostic association, once adjusted for the standard clinico-pathological variables, might be explained by the association of TIL with poor prognostic features. Of interest, in the BIG 02-98 study, we observed at the univariate level that high TIL were associated with worse prognosis in ILC, although without reaching statistical significance. Interestingly, in this study, TIL did not show any association with survival in ER-positive/HER2-negative IDC.

When we compared the immuno-histochemical scores (total, intra-tumoral, adjacent stromal and distant stromal) of the $CD3^+$, $CD4^+$, $CD8^+$, $CD68^+$ and $FOXP3^+$ cells on the Nottingham series between these two main breast cancer histologies, we noticed that while no difference was observed for total $CD8^+$ levels, intra-tumoral $CD8^+$ levels were statistically significantly lower in ER-positive/HER2-negative ILC compared to IDC, with very rare ILC cases presenting with intra-tumoral $CD8^+$ cells, suggesting that ILC might present an immune-excluded phenotype where immune cells are retained in the stroma therefore limiting cancer immunity. Since tumors with intra-tumoral $CD8^+$ cells have been associated with the best outcome (41), ILC tumors with high TIL levels might be associated with a worse prognosis because of the lack of intra-tumoral $CD8^+$ cells. While the initial transcriptomic comparison between the low and high-infiltrated groups showed similarities with previously reported immune signatures, the CIBERSORT analyses further revealed statistically significant differences in immune composition between infiltrated ER-positive/HER2-negative IDC and ILC tumors. Whether the strong underrepresentation of M1 macrophages or follicular helper T cells in ILC compared to IDC could further explain our prognostic observations needs to be further investigated.

A unique advantage of our retrospective cohort was the ability to investigate the association between genomic alterations and TIL. Tumors presenting *ARID1A*, *BRCA2* and *TP53* mutations, as well as 8q24.23 loss and 7p21.2 gains were associated with higher TIL counts. Although we could not find previous evidence for the association of *ARID1A* mutations and TIL in breast cancer, a study of hepatocellular carcinoma demonstrated that hepatocyte-specific deficiency of *ARID1A* lead to the infiltration of innate immune cells (42). Similarly, in colorectal cancer, *ARID1A* mutations are known to be more frequent in microsatellite-instable tumors and these tumors are also associated with a higher

immune expression scores (43). It has to be noted however that *ARID1A* mutations were previously demonstrated to be enriched in ER-positive/HER2-negative ILC (~6%) compared to ER-positive/HER2-negative IDC (<2%) (13). Regarding *BRCA2*, our observation is in line with the study of Bane *et al.* which reported that *BRCA2*-mutated tumors exhibited lymphocytic infiltration at the periphery of the tumor (44). Whilst *TP53* mutations have been shown to be associated with higher levels of TIL in ovarian cancer (45), lymphocytic infiltration in basal-like breast cancer has only recently been reported to be associated with the retention of wild type *TP53* (46). While some evidence is now beginning to accumulate pertaining to the clinical utility of mutation burden, the role of TIL and genomic alterations as potential biomarkers for immunotherapy needs to be further investigated.

We recognize that this study has limitations, which are mainly due to its retrospective nature and the clinically and pathologically heterogeneity of the cohorts that were analyzed. Nevertheless, this study represents to the best of our knowledge the largest study investigating immune infiltration in ILC.

To conclude, we have shown, in a large cohort and using a standardized methodology for TIL assessment, that most ILC were characterized by generally low but variable levels of lymphocytic infiltration. We further demonstrated that higher TIL levels were associated with worse prognosis in ILC but only at the univariable level. The association of TIL with outcome in ER-positive/HER2-negative breast cancer patients should be further investigated in additional large trials to understand whether the association is limited to ILC or not, and whether high lymphocytic infiltration could drive endocrine resistance as previously suggested (47). We further highlighted several differences in terms of immune composition and localization between ILC and IDC, suggestive of an immune-exclusion phenotype. Finally, we showed that higher TIL levels were found in association with specific mutations and copy number alterations. Overall, these observations suggest that that immune infiltration could play a different role in ILC compared to IDC. Further research is needed to understand whether and how immunomodulators could reestablish and promote the anti-tumor immune response in ILC.

References

1. Savas P, Salgado R, Denkert C, et al. Clinical relevance of host immunity in breast cancer: from TILs to the clinic. *Nat Rev Clin Oncol*. 2015;13(4):228-241.

2. Pruneri G, Vingiani A, Denkert C. Tumor infiltrating lymphocytes in early breast cancer. *The Breast*. 2017.

3. Stanton SE, Adams S, Disis ML, DJ S, WD F, TO N. Variation in the Incidence and Magnitude of Tumor-Infiltrating Lymphocytes in Breast Cancer Subtypes. *JAMA Oncol*. 2016;2(10):1354.

4. Salgado R, Denkert C, Demaria S, et al. The evaluation of tumor-infiltrating lymphocytes (TILs) in breast cancer: recommendations by an International TILs Working Group 2014. *Ann Oncol*. 2014;26(2):259-271.

5. Buisseret L, Desmedt C, Garaud S, et al. Reliability of tumor-infiltrating lymphocyte and tertiary lymphoid structure assessment in human breast cancer. *Mod Pathol*. 2017; 30(9):1204-1212.

6. Newman AM, Liu CL, Green MR, et al. Robust enumeration of cell subsets from tissue expression profiles. *Nat Methods*. 2015;12(5):453-457.

7. Ali HR, Chlon L, Pharoah PDP, Markowetz F, Caldas C. Patterns of Immune Infiltration in Breast Cancer and Their Clinical Implications: A Gene-Expression-Based Retrospective Study. *PLoS Med*. 2016:1-24.

8. Bense RD, Sotiriou C, Piccart-Gebhart MJ, et al. Relevance of Tumor-Infiltrating Immune Cell Composition and Functionality for Disease Outcome in Breast Cancer. *J Natl Cancer Inst*. 2017;109(1):djw192.

9. Guiu S, Wolfer A, Jacot W, et al. Invasive lobular breast cancer and its variants: how special are they for systemic therapy decisions? *Crit Rev Oncol Hematol*. 2014;92(3):235-257.

10. Pestalozzi BC, Zahrieh D, Mallon E, et al. Distinct clinical and prognostic features of infiltrating lobular carcinoma of the breast: combined results of 15 International Breast Cancer Study Group

clinical trials. *J Clin Oncol*. 2008;26(18):3006-3014.

11. Ciriello G, Gatza ML, Beck AH, et al. Comprehensive Molecular Portraits of Invasive Lobular Breast Cancer. *Cell*. 2015;163(2):506-519.

12. Michaut M, Chin SF, Majewski I, et al. Integration of genomic, transcriptomic and proteomic data identifies two biologically distinct subtypes of invasive lobular breast cancer. *Sci Rep*. 2016;6:18517.

13. Desmedt C, Zoppoli G, Gundem G, et al. Genomic Characterization of Primary Invasive Lobular Breast Cancer. *J Clin Oncol*. 2016;34(16):1872-1881.

14. Pereira B, Chin SF, Rueda OM, et al. The somatic mutation profiles of 2,433 breast cancers refines their genomic and transcriptomic landscapes. *Nat Commun*. 2016;7:11479.

15. Loi S, Sirtaine N, Piette F, et al. Prognostic and predictive value of tumor-infiltrating lymphocytes in a phase III randomized adjuvant breast cancer trial in node-positive breast cancer comparing the addition of docetaxel to doxorubicin with doxorubicin-based chemotherapy: BIG 02-98. *J Clin Oncol*. 2013;31(7):860-867.

16. Mahmoud SM, Lee AH, Paish EC, Macmillan RD, Ellis IO, Green AR. The prognostic significance of B lymphocytes in invasive carcinoma of the breast. *Breast Cancer Res Treat*. 2011;132(2):545-553.

17. Mahmoud SM, Lee AH, Paish EC, Macmillan RD, Ellis IO, Green AR. Tumour-infiltrating macrophages and clinical outcome in breast cancer. *J Clin Pathol*. 2011;65(2):159-163.

18. Mahmoud SM, Paish EC, Powe DG, et al. An evaluation of the clinical significance of FOXP3+ infiltrating cells in human breast cancer. *Breast Cancer Res Treat*. 2011;127(1):99-108.

19. Curtis C, Shah SP, Chin SF, et al. The genomic and transcriptomic architecture of 2,000 breast tumours reveals novel subgroups. *Nature*. 2012;486(7403):346-352.

20. Sonnenblick A, Francis PA, Azim Jr. HA, et al. Final 10-year results of the Breast International

Group 2-98 phase III trial and the role of Ki67 in predicting benefit of adjuvant docetaxel in patients with oestrogen receptor positive breast cancer. *Eur J Cancer*. 2015;51(12):1481-1489.

21. Shrout PE FJL. Intraclass Correlations : Uses in Assessing Rater Reliability. *Psychol Bull*. 1979;86(2):420-428.

22. Passing H, Bablok. A new biometrical procedure for testing the equality of measurements from two different analytical methods. Application of linear regression procedures for method comparison studies in clinical chemistry, Part I. *J Clin Chem Clin Biochem*. 1983;21(11):709-720.

23. Box GE CD. An analysis of transformations. *J R Stat Soc Ser B*. 1964:211-252.

24. Harrell FE. Regression modeling strategies: with applications to linear models, logistic and ordinal regression, and survival analysis. *Springer*. 2001:307. doi:10.1007/978-1-4757-3462-1.

25. Benjamini Yosef YH. Controlling the false discovery rate: a practical and powerful approach to multiple testing. *J R Stat Soc Ser B*. 1995;57(1):289-300.

26. R Core Team. R: A Language and Environment for Statistical Computing. *R Found Stat Comput Vienna, Austria*. 2017;0:{ISBN} 3-900051-07-0. doi:http://www.R-project.org/.

27. Desmedt C, Fumagalli D, Pietri E, et al. Uncovering the genomic heterogeneity of multifocal breast cancer. *J Pathol*. 2015;236(4):457-466.

28. Desmedt C, Haibe-Kains B, Wirapati P, et al. Biological processes associated with breast cancer clinical outcome depend on the molecular subtypes. *Clin Cancer Res*. 2008;14(16):5158-5165.

29. Teschendorff AE, Miremadi A, Pinder SE, Ellis IO, Caldas C. An immune response gene expression module identifies a good prognosis subtype in estrogen receptor negative breast cancer. *Genome Biol*. 2007;8(8):R157.

30. Bild AH, Yao G, Chang JT, et al. Oncogenic pathway signatures in human cancers as a guide to targeted therapies. *Nature*. 2006;439(7074):353-357.

31. Saal LH, Johansson P, Holm K, et al. Poor prognosis in carcinoma is associated with a gene expression signature of aberrant PTEN tumor suppressor pathway activity. *Proc Natl Acad Sci U S A*. 2007;104(18):7564-7569.

32. Majumder PK, Febbo PG, Bikoff R, et al. mTOR inhibition reverses Akt-dependent prostate intraepithelial neoplasia through regulation of apoptotic and HIF-1-dependent pathways. *Nat Med*. 2004;10(6):594-601.

33. Creighton CJ, Hilger AM, Murthy S, Rae JM, Chinnaiyan AM, El-Ashry D. Activation of mitogen-activated protein kinase in estrogen receptor alpha-positive breast cancer cells in vitro induces an in vivo molecular phenotype of estrogen receptor alpha-negative human breast tumors. *Cancer Res*. 2006;66(7):3903-3911.

34. Creighton CJ. A gene transcription signature of the Akt/mTOR pathway in clinical breast tumors. *Oncogene*. 2007;26(32):4648-4655.

35. Der SD, Zhou A, Williams BRG, Silverman RH. Identification of genes differentially regulated by interferon alpha, beta, or gamma using oligonucleotide arrays. *Proc Natl Acad Sci*. 1998;95(26):15623-15628.

36. Gu-Trantien C, Loi S, Garaud S, et al. CD4(+) follicular helper T cell infiltration predicts breast cancer survival. *J Clin Invest*. 2013;123(7):2873-2892.

37. Alexe G, Dalgin GS, Scanfeld D, et al. High expression of lymphocyte-associated genes in node-negative HER2+ breast cancers correlates with lower recurrence rates. *Cancer Res*. 2007;67(22):10669-10676.

38. Ali HR, Provenzano E, Dawson SJ, et al. Association between CD8+ T-cell infiltration and breast cancer survival in 12,439 patients. *Ann Oncol*. 2014;25(8):1536-1543.

39. Yamaguchi R, Tanaka M, Yano A, et al. Tumor-infiltrating lymphocytes are important pathologic predictors for neoadjuvant chemotherapy in patients with breast cancer. *Hum Pathol*. 2012;43(10):1688-1694.

40. Droeser R, Zlobec I, Kilic E, et al. Differential pattern and prognostic significance of CD4+, FOXP3+ and IL-17+ tumor infiltrating lymphocytes in ductal and lobular breast cancers. *BMC Cancer*. 2012;12:134.

41. Ali HR, Provenzano E, Dawson SJ, et al. Association between CD8+ T-cell infiltration and breast cancer survival in 12 439 patients. *Ann Oncol*. 2014;25(8):1536-1543.

42. Fang JZ, Li C, Liu XY, Hu TT, Fan ZS, Han ZG. Hepatocyte-Specific Arid1a Deficiency Initiates Mouse Steatohepatitis and Hepatocellular Carcinoma. *PLoS One*. 2015;10(11):e0143042.

43. Mlecnik B Angell HK, Maby P, Angelova M, Tougeron D, Church SE, BG, Lafontaine L Fredriksen T, Sasso M, Bilocq AM, Kirilovsky A, Obenauf FM, AC Berger A, Bruneval P, Tuech JJ, Sabourin JC, Le Pessot F, Mauillon HM, J Laurent-Puig P, Speicher MR, Trajanoski Z, Michel P, Sesboüe R, RA, Frebourg T Valge-Archer V, Latouche JB, Galon J PF. Integrative Analyses of Colorectal Cancer Show Immunoscore Is a Stronger Predictor of Patient Survival Than Microsatellite Instability. *Cell*. 2016;44(3):698-711.

44. Bane AL, Beck JC, Bleiweiss I, et al. BRCA2 mutation-associated breast cancers exhibit a distinguishing phenotype based on morphology and molecular profiles from tissue microarrays. *Am J Surg Pathol*. 2007;31(1):121-128.

45. Shah CA, Allison KH, Garcia RL, Gray HJ, Goff BA, Swisher EM. Intratumoral T cells, tumor-associated macrophages, and regulatory T cells: association with p53 mutations, circulating tumor DNA and survival in women with ovarian cancer. *Gynecol Oncol*. 2008;109(2):215-219.

46. Quigley D, Silwal-Pandit L, Dannenfelser R, et al. Lymphocyte Invasion in IC10/Basal-Like Breast Tumors Is Associated with Wild-Type TP53. *Mol Cancer Res*. 2015;13(3):493-501.

47. Dunbier AK, Ghazoui Z, Anderson H, et al. Molecular Profiling of Aromatase Inhibitor-Treated Postmenopausal Breast Tumors Identifies Immune-Related Correlates of Resistance. *Clin Cancer Res*. 2013;19(10):2775-2786.

Funding

This work was supported by Susan Komen for the Cure, Fondation MEDIC, Les Amis de Bordet (C.D.), Fonds National de Recherche Scientifique (D.B. and C.S.), the Cancer Council Victoria John Colebatch fellowship (S.L.), the Breast Cancer Research Foundation (BCRF), the Italian Association for Leukemia and Lymphoma (AIL), and the Italian Association for Cancer Research (AIRC). We thank the Nottingham Health Science Biobank and Breast Cancer Now Tissue Bank, as well as the bio-banks from the Institut Jules Bordet, the European Institute of Oncology, the Sint Augustinus Hospital, the Cliniques universitaires de Saint Luc and the Institut Paoli-Calmettes for the provision of tissue samples. BIG 2-98 was conducted under the umbrella of the Breast international group (BIG), with sponsorship and funding provided by Sanofi.

Notes

The funders had no role in the design of the study; the collection, analysis, and interpretation of the data; the writing of the manuscript; and the decision to submit the manuscript for publication.

Part of this work has been presented orally at the annual San Antonio Breast Cancer Symposium in December 2015 (Desmedt *et al.* S1-02).

Author Contributions: Drs Desmedt, Biganzoli and Sotiriou had full access to all the data in the study and take responsibility for the integrity of the data and the accuracy of the data analysis. Drs Biganzoli and Sotiriou are joint senior authors.

Study concept and design: Desmedt, Biganzoli, Sotiriou

Acquisition, analysis, or interpretation of data: all authors

Drafting of the manuscript: Desmedt, Biganzoli, Sotiriou

Critical revision of the manuscript for important intellectual content: all authors.

Statistical analysis: Fornili, Bareche, Biganzoli

Obtained funding: Desmedt, Sotiriou

Administrative, technical, or material support: Garaud, Rouas

Study supervision: Desmedt, Biganzoli, Sotiriou.

Conflict of Interest Disclosures

SL received contracted research funding directly to her institute from Novartis, Pfizer, Merck, Genentech/Roche, Puma Biotechnology and Bristol-Myers Squibb. No disclosures are reported for the other authors.

Figure legends

Figure 1: Distribution of Tumor Infiltrating Lymphocytes

Histograms displaying the distribution of the TIL counts in all ILC cases, and only in the ER-positive/HER2-negative ones (A), as well as the distribution of ER-positive/HER2-negative ILC and IDC cases from the BIG 02-98 study (B).

ER: estrogen receptor, IDC: invasive ductal carcinoma, ILC: invasive lobular carcinoma, TIL: Tumor Infiltrating Lymphocyte.

Figure 2: Associations between Tumor Infiltrating Lymphocytes and clinico-pathological variables

Univariable and multivariable associations between TIL and clinico-pathological variables in all ILC cases and only the ER-positive/HER2-negative from our series (A), as well as from the ER-positive/HER2-negative ILC and IDC (B) from the BIG 02-98 study.

ER: estrogen receptor, IDC: invasive ductal carcinoma, ILC: invasive lobular carcinoma, TIL: Tumor Infiltrating Lymphocyte.

Figure 3: Associations between Tumor Infiltrating Lymphocytes, genomic and transcriptomic features in the retrospective ILC cohort

Univariable and multivariable associations between TIL and recurrently mutated genes (n=399) (A) or recurrent CNAs (n=166) (B). Heatmap of the genes statistically significantly associated with TIL at the transcriptomic level (C). Correlation matrix of the lobular immune gene expression signature (ILC TIL) with published immune signatures (D).

CAN: copy number aberration, ILC: invasive lobular carcinoma, TIL: Tumor Infiltrating Lymphocyte.

Figure 4: Comparison of the expression of various immune cell types between ER-positive/HER2-negative ILC

Distribution of the expression of the various immune markers assessed by immuno-histochemistry in the Nottingham cohort according to the histology and their localization. For each comparison, the value in parenthesis refers to the multivariable adjusted *P*-value from proportional odds logistic model extension of the Mann-Whitney test according to Harrell (24) with the following covariates: histological subtype, age, grade, axillary lymph node and Ki67 status.

ER: estrogen receptor, ILC: invasive lobular carcinoma.

Figure 5: Association between TIL and survival

Kaplan-Meier curves displaying the estimated breast cancer-free interval probability according to the TIL group (low: ≤ 5%, intermediate: > 5 and ≤ 10%, high: >10%) in all ILC (A) and only the ER-positive/HER2-negative ILC of the retrospective series (B). Kaplan-Meier curves displaying the estimated disease-free survival probability according to the TIL group in all ILC (C) and only the ER-positive/HER2-negative ILC (D) from the BIG 02-98 series. All statistical tests were two-sided.

ER: estrogen receptor, ILC: invasive lobular carcinoma, TIL: Tumor Infiltrating Lymphocyte.

Supplementary Material

Immune infiltration in invasive lobular breast cancer

Desmedt *et al.*

Supplementary Figures

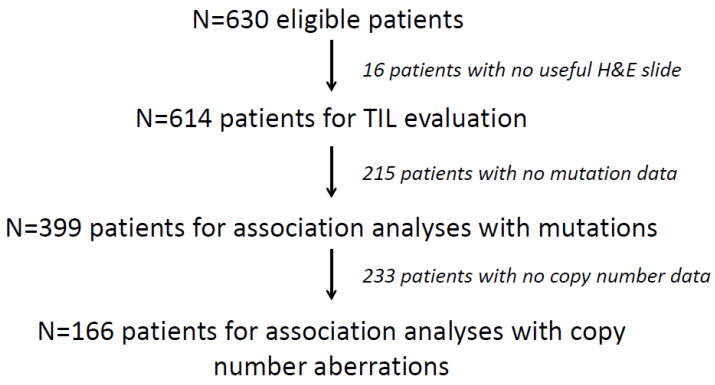

Supplementary Figure 1: Flow diagram representing the number of patients considered for the various analyses in the multi-centric retrospective lobular cohort.

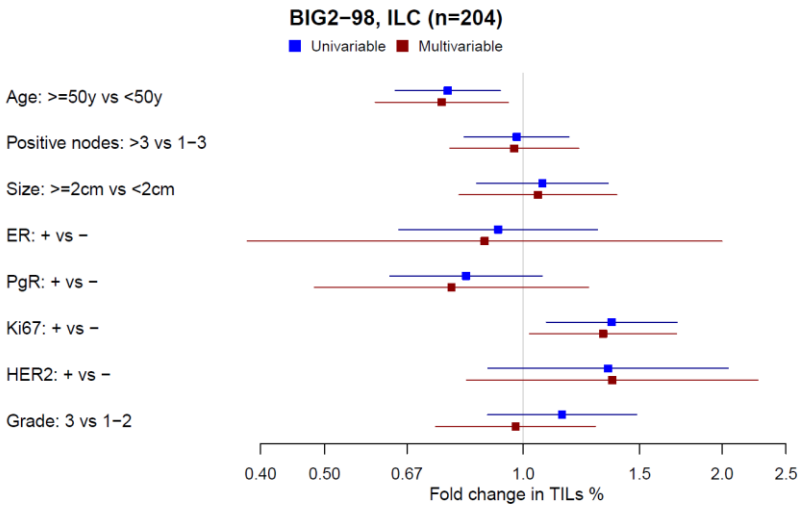

Supplementary Figure 2: Univariable and multivariable associations between TIL and clinico-pathological variables in all ILC cases from the BIG 2-98 study.

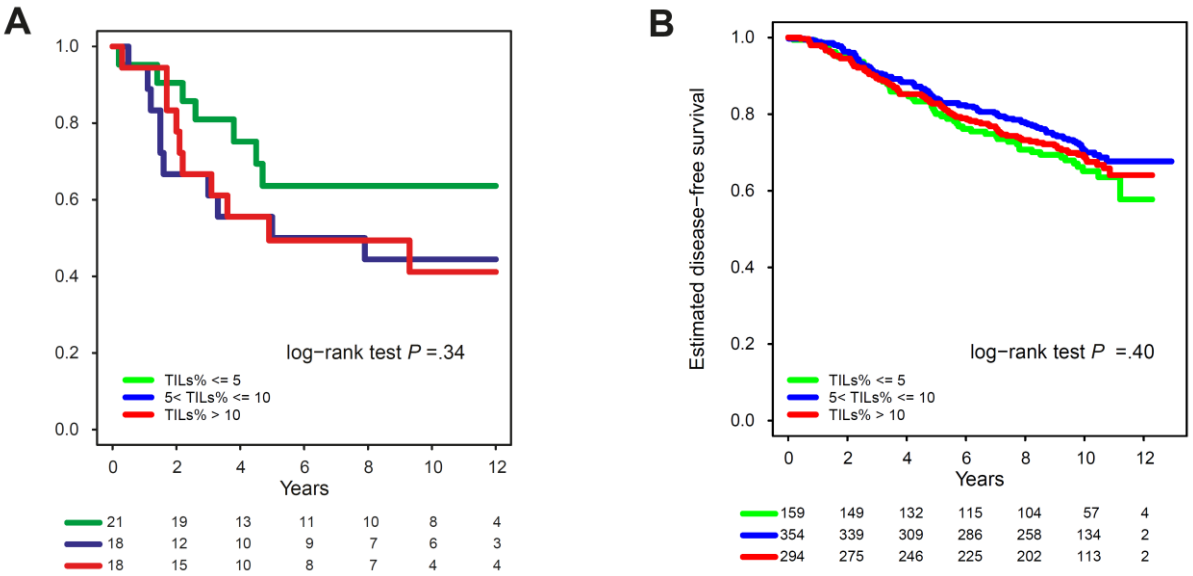

Supplementary Figure 3: Kaplan-Meier curves displaying the estimated breast cancer-free interval probability according to the TIL group (low: ≤ 5%, intermediate: > 5 and ≤ 10%, high: >10%) in the ER-negative and/or HER2-positive ILC from the retrospective cohort (A), and the estimated disease-free survival probability according to the TIL group in all ER-positive/HER2-negative IDC from the BIG 2-98 series (B). The statistical test was two-sided. ER: estrogen receptor, IDC: invasive ductal carcinoma, ILC: invasive lobular carcinoma, TIL: Tumor Infiltrating Lymphocyte.

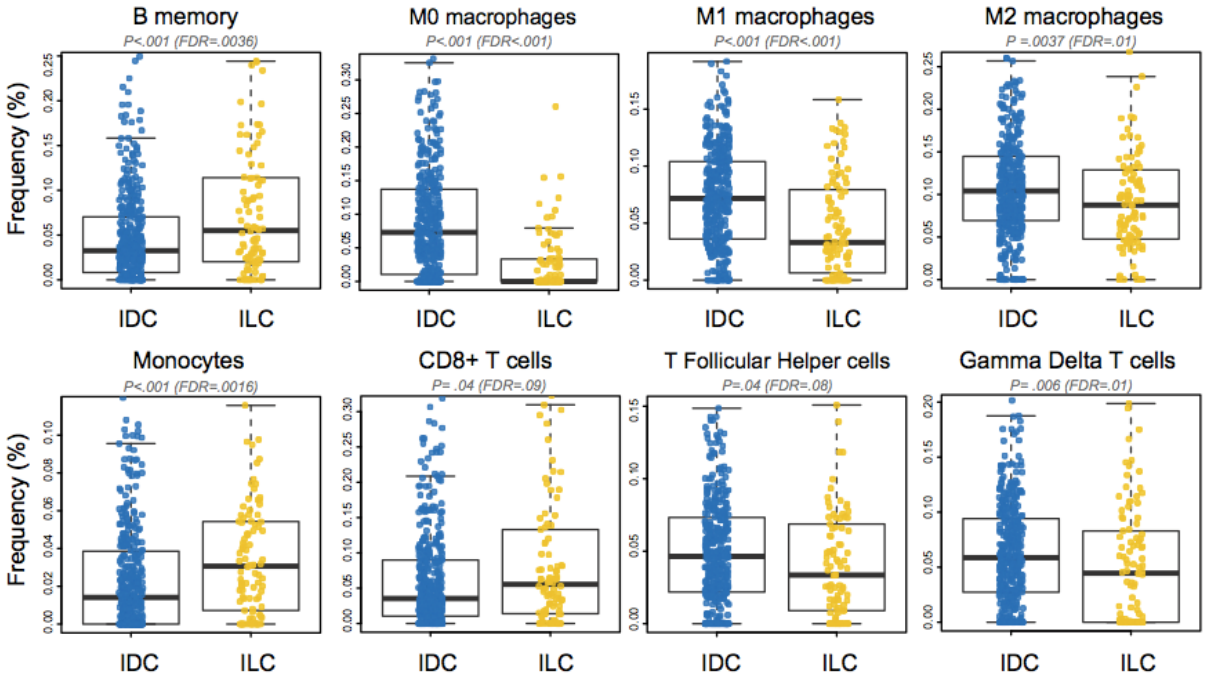

Supplementary Figure 4: Distribution of the frequency of the eight immune populations that differed significantly (FDR<0.10) between the combined ER-positive/HER2-negative ILC and IDC tumors from METABRIC and TCGA. *P*-values were computed using the Wilcoxon rank sum test and were two-sided. ER: estrogen receptor, IDC: invasive ductal carcinoma, ILC: invasive lobular carcinoma.

3. Supplementary Tables

Supplementary Table 1: Global ILC patient and sample characteristics from the multi-centric retrospective series

Characteristic	No. of patients	% of patients
Age (years)		
<50	201	32.7
≥50	413	67.3
Tumor size (cm)		
< 2	248	40.4
≥ 2	366	59.6
Nodal status		
Negative	296	50.0
Positive	296	50.0
Unknown	22	
Tumor Grade		
Grade 1	76	12.5
Grade 2	438	71.9
Grade 3	95	15.6
Unknown	5	
Ki67 status		
< 20%	416	68.6
≥ 20%	190	31.4
Unknown	8	
Receptor status*		
ER-	37	6.0
ER+/PgR-	115	18.8
ER+/PgR+	461	75.2
Unknown	1	
HER2 status*		
Negative	585	95.6
Positive	27	4.4
Unknown	2	
Histological subtype		
Alveolar	100	16.3
Classic	301	49.0
Mixed, non-classic	91	14.8
Solid	89	14.5
Trabecular	33	5.4

* The ER and HER2 status denote the pathological assessment by immunohistochemistry (IHC) and combined IHC/FISH status of these markers.

<u>Supplementary Table 2</u>: ILC patient and sample characteristics (including TIL) from the multi-centric retrospective series

ID	Center	Age	BCFI	BCFI event	Subtype	Size (cm)	Positive nodes	ER	PgR	HER2	Ki67	Grade	TIL
PD9896c	1	69	4,2	No	Classic	2,5	0	Positive	Positive	Negative	1	2	6
PD13045c	1	54	4,5	Yes	Classic	4,1	17	Positive	Positive	Negative	5	2	20
PD13046a	1	64	11,5	No	Classic	2,1	0	Negative	Positive	Negative	5	1	3
PD13047a	1	66	2,1	Yes	Classic	5,1	0	Positive	Positive	Negative	10	1	10
PD13048a	1	66	12	No	Classic	2,8	0	Negative	Positive	Negative	1	1	6
PD13049a	1	70	12,1	No	Classic	2,3	1	Negative	Negative	Negative	10	2	12
PD9871c	1	88	7,7	No	Classic	5	0	Positive	Negative	Negative	4	1	1
PD9857d	1	52	3,3	Yes	Classic	5,1	4	Positive	Positive	Negative	18	2	6
PD9863c	1	67	11	No	Alveolar	2,3	0	Positive	Positive	Negative	10	2	4
PD9858c	1	49	15	No	Classic	1,3	0	Negative	Negative	Negative	2	2	9
PD9895c	1	74	14	No	Classic	1,3	0	Positive	Positive	Negative	47	2	8
PD9872d	1	76	7,8	No	Solid	1,9	0	Positive	Positive	Negative	8	2	3
PD9862d	1	62	3,3	Yes	Trabecular	2,3	0	Negative	Positive	Positive	25	2	6
PD13051c	1	65	9,4	No	Classic	7	0	Positive	Positive	Negative	10	2	4
PD13052a	1	58	10,1	No	Classic	5,1	0	Positive	Negative	Negative	10	2	40
PD9884d	1	45	9,3	No	Trabecular	1,3	0	Positive	Positive	Negative	30	2	65
PD9912c	1	49	9,3	No	Classic	2,3	0	Positive	Positive	Negative	10	1	4
PD13053a	1	66	1,2	Yes	Trabecular	2,3	13	Positive	Negative	Negative	15	2	4
PD13054a	1	65	10,3	No	Classic	2,6	0	Positive	Negative	Negative	1	2	3
PD13055a	1	57	4,5	No	Classic	9	0	Positive	Negative	Negative	10	2	2
PD13056a	1	51	5	Yes	Classic	5,1	1	Negative	Negative	Negative	10	2	10
PD13057a	1	57	13,9	Yes	Classic	2,3	22	Positive	Negative	Negative	14	2	4
PD9910d	1	79	5,5	No	Classic	4,2	0	Positive	Negative	Negative	5	2	15
PD9911c	1	52	9,6	No	Classic	1,4	0	Positive	Positive	Negative	10	2	5
PD13059c	1	54	15,8	No	Classic	3,5	1	Negative	Positive	Negative	1	2	1
PD9906c	1	57	2	Yes	Classic	2	4	Positive	Negative	Negative	31	2	8
PD9907c	1	50	14,9	No	Classic	7	9	Positive	Positive	Negative	10	2	5
PD9913c	1	46	9,1	No	Classic	1,9	0	Positive	Positive	Negative	10	2	20
PD13060c	1	51	7,1	No	Classic	1,7	3	Positive	Positive	Negative	5	2	15
PD13061c	1	65	5,8	Yes	Classic	1,8	0	Positive	Positive	Negative	5	2	11
PD9914d	1	52	8,4	No	Classic	3,5	0	Positive	Positive	Negative	10	2	9
PD9886d	1	36	7,9	Yes	Classic	1,4	1	Positive	Positive	Negative	10	2	7
PD9915c	1	54	8	No	Classic	1,7	1	Positive	Positive	Negative	9	2	2
PD13062c	1	77	7,9	No	Mixed, non classic	3,3	5	Positive	Positive	Positive	10	3	6
PD13063a	1	46	7,6	No	Classic	2,3	3	Positive	Positive	Negative	5	2	4
PD9892d	1	66	10,9	No	Classic	3,5	0	Negative	Positive	Negative	2	1	6
PD13064c	1	58	13,8	No	Classic	6	2	Positive	Positive	Negative	15	2	7
PD13065a	1	64	5,3	Yes	Classic	2	7	Positive	Positive	Negative	23	2	4
PD13067c	1	58	4,7	No	Classic	2,2	0	Positive	Positive	Negative	5	2	6
PD13068a	1	48	7,5	No	Classic	4	2	Positive	Positive	Negative	10	2	9
PD13069c	1	44	12,8	No	Classic	1,1	0	Positive	Positive	Negative	4	2	5

PD13070a	1	51	13,2	Yes	Classic	5	0	Positive	Negative	Negative	19	2	4
PD9893c	1	55	16,1	No	Classic	3	0	Positive	Positive	Negative	1	2	7
PD13071c	1	65	12,7	No	Classic	2,4	3	Positive	Positive	Negative	31	2	4
PD13072a	1	59	13,5	No	Classic	3	0	Positive	Negative	Negative	2	2	10
PD13073a	1	54	1,3	Yes	Solid	7	3	Positive	Negative	Negative	21	3	2
PD13074a	1	58	12,8	No	Trabecular	2	1	Positive	Positive	Negative	30	3	12
PD13075a	1	69	5,1	No	Classic	3,2	0	Positive	Positive	Negative	3	2	10
PD13076a	1	53	10,6	No	Classic	4	0	Positive	Negative	Negative	2	2	4
PD13077c	1	77	3,9	No	Classic	1,5	2	Positive	Negative	Negative	15	2	6
PD13078c	1	50	12,9	No	Classic	9	2	Positive	Positive	Negative	4	1	5
PD9869d	1	69	15,1	No	Solid	2	0	Positive	Negative	Negative	54	2	15
PD13079a	1	63	9,9	No	Classic	5	10	Positive	Negative	Negative	10	2	6
PD13080c	1	61	1,7	Yes	Solid	2,6	18	Positive	Positive	Positive	20	3	14
PD13081a	2	48	9,9	No	Classic	1,6	0	Positive	Positive	Negative	5	2	2
PD13082c	2	61	9,6	No	Classic	5,5	5	Positive	Positive	Negative	5	2	3
PD13083a	2	52	10,3	No	Classic	5	0	Positive	Positive	Negative	5	1	2
PD13084a	2	54	8,6	No	Classic	1,5	0	Positive	Negative	Negative	5	1	4
PD13086a	2	59	1,1	Yes	Classic	9	10	Positive	Positive	Negative	10	2	2
PD9894c	1	52	6,2	No	Classic	3	0	Positive	Positive	Negative	26	2	4
PD13088a	2	48	8,3	No	Classic	1,2	0	Positive	Positive	Negative	20	2	4
PD13089a	2	43	7,7	Yes	Trabecular	1,4	0	Positive	Positive	Negative	25	2	6
PD13090a	2	52	7,3	No	Trabecular	2,9	1	Positive	Positive	Negative	30	2	4
PD13091a	3	75	1,5	Yes	Mixed, non classic	5	3	Negative	Negative	Negative		2	7
PD13092a	1	47	15	No	Trabecular	3	10	Positive	Negative	Negative	1	2	20
PD13094a	3	85	1,9	Yes	Classic	7	10	Positive	Negative	Negative	10	2	1
PD13095a	3	69	3,9	Yes	Solid	10	3	Positive	Positive	Negative	60	3	1
PD13096a	3	59	4,1	Yes	Classic	3,6	0	Positive	Positive	Negative	15	2	2
PD13098a	3	55	10,2	No	Classic	2	1	Positive	Positive	Negative	1	2	6
PD13099a	3	43	6,5	Yes	Classic	9	10	Positive	Positive	Negative	20	2	5
PD13100a	3	77	7	No	Classic	2,5	0	Positive	Positive	Negative		1	3
PD9859c	1	58	14,4	No	Solid	3,5	0	Positive	Positive	Negative	21	2	8
PD13101a	3	68	8,3	No	Trabecular	2	1	Positive	Negative	Negative	20	2	4
PD13102a	3	78	9,3	No	Classic	5	0	Positive	Negative	Negative	5	1	10
PD13103c	3	85	5	Yes	Trabecular	3	1	Positive	Positive	Negative		2	6
PD13104a	3	62	8	No	Classic	4,5	0	Positive	Positive	Negative	1	2	45
PD13106a	1	71	13	No	Solid	2	0	Positive	Negative	Negative	1	2	5
PD13107a	3	60	9	No	Classic	1,2	0	Positive	Positive	Negative		2	15
PD13108a	3	60	7,3	No	Classic	5	1	Positive	Positive	Negative	1	2	4
PD13109a	3	62	9,1	No	Classic	4,2	1	Positive	Positive	Negative	5	2	40
PD13111a	3	56	10,1	No	Classic	7,6	3	Positive	Negative	Negative	30	2	4
PD13112a	3	55	6,8	No	Trabecular	2,8	3	Positive	Negative	Negative	40	2	90
PD13113a	3	55	7,4	No	Classic	4	0	Positive	Positive	Negative	1	2	2
PD13114a	3	58	8,2	No	Classic	3,7	0	Positive	Negative	Negative	15	2	10
PD13115a	3	65	4,4	Yes	Classic	2,5	20	Positive	Positive	Negative	5	2	30
PD13116a	3	55	9,2	No	Classic	2	0	Positive	Positive	Negative	50	2	4

PD13117a	3	46	4,8	Yes	Trabecular	5	5	Positive	Positive	Negative	30	3	6
PD13118a	3	72	5,1	Yes	Classic	10	2	Positive	Positive	Negative	40	2	20
PD13120a	3	69	10,1	No	Classic	1,8	0	Positive	Positive	Negative	5	1	1
PD9865f	1	56	1,2	Yes	Classic	2,5	0	Positive	Negative	Negative	20	2	28
PD13121a	3	42	10,9	No	Classic	17	4	Positive	Negative	Negative	5	2	10
PD13122a	3	58	4,9	Yes	Trabecular	5	18	Positive	Positive	Negative	50	3	6
PD13123a	3	75	1,2	Yes	Solid	4	11	Negative	Negative	Negative	30	3	6
PD13124a	3	79	0,3	Yes	Classic	9		Negative	Negative	Negative	20	2	25
PD13127a	3	68	11	No	Solid	2	0	Negative	Negative	Negative	30	3	5
PD13128a	3	80	3,5	No	Classic	11	0	Negative	Negative	Negative	15	2	1
PD13129a	3	53	4,6	Yes	Classic	2	0	Positive	Positive	Negative	50	2	1
PD13130a	3	84	5,8	No	Classic	1,8	0	Positive	Positive	Negative		1	6
PD13131a	1	69	10,1	No	Classic	1,1	0	Positive	Positive	Negative	5	2	7
PD9898c	1	58	8,6	No	Classic	1,7	0	Positive	Positive	Negative	15	2	15
PD9897d	1	53	10,2	No	Classic	2,4	1	Positive	Positive	Negative	10	1	4
PD9866c	1	49	9,1	No	Classic	1,1	0	Positive	Positive	Negative	9	2	7
PD9890c	1	66	3	Yes	Classic	6	6	Positive	Negative	Positive	40	2	6
PD13132a	1	82	9,1	No	Classic	3	0	Positive	Positive	Negative		2	3
PD9900c	1	59	9,5	No	Classic	0,8	0	Positive	Negative	Positive	15	2	6
PD13133a	1	79	7,5	No	Solid	2	1	Positive	Positive	Negative	10	2	3
PD13134c	1	40	7,2	No	Classic	1,1	0	Positive	Positive	Negative	10	1	4
PD9888d	1	34	10,9	Yes	Trabecular	3,5	8	Positive	Positive	Negative	34	2	10
PD9873c	1	59	8,5	No	Classic	2,3	0	Positive	Positive	Negative	9	2	4
PD9874c	1	59	9,1	No	Alveolar	2,8	0	Positive	Positive	Negative	5	2	4
PD13135c	1	54	8,7	No	Classic	4	0	Positive	Positive	Negative	5	1	5
PD9876c	1	77	8,2	No	Classic	1,4	0	Positive	Positive	Negative	10	2	7
PD9901c	1	70	7,3	No	Classic	2,5	0	Positive	Positive	Negative	9	1	13
PD13138c	1	69	5,5	No	Classic	2,5	2	Positive	Positive	Negative	9	2	4
PD13139a	1	69	9,7	Yes	Solid	3	2	Positive	Negative	Negative	10	3	4
PD13140c	1	48	8	No	Classic	10	0	Positive	Negative	Negative	10	2	9
PD9903d	1	40	4,6	No	Classic	6	4	Positive	Positive	Negative	10	3	6
PD9902c	1	51	1,5	No	Classic	0,9	0	Positive	Positive	Negative	5	2	13
PD13142a	1	69	2,5	No	Classic	2,5	0	Positive	Positive	Negative	10	2	11
PD13143c	1	80	12,8	No	Trabecular	2	0	Positive	Negative	Negative	5	2	4
PD9868c	1	45	16,4	No	Mixed, non classic	3	1	Positive	Positive			3	5
PD9889g	1	40	5,5	Yes	Classic	6	1	Positive	Positive	Negative	4	1	7
PD13145a	1	57	12,2	No	Classic	2,1	0	Positive	Positive	Negative	5	1	4
PD13146c	1	50	9,1	No	Trabecular	3	0	Positive	Negative	Negative	5	2	2
PD13147a	1	40	8,5	No	Classic	2,2	3	Positive	Positive	Negative	10	2	10
PD13148a	1	67	7,3	Yes	Classic	1,7	0	Positive	Positive		18	2	7
PD13149c	1	49	5,1	No	Classic	2,5	0	Positive	Positive	Negative	50	2	3
PD13150a	1	62	2,9	No	Classic	1,6	0	Positive	Positive	Negative	10	2	4
PD9867d	1	40	7,9	Yes	Classic	2,5	2	Negative	Positive	Negative	11	1	10
PD13151a	1	60	17,8	No	Trabecular	1,8	1	Positive	Positive	Negative	54	2	2
PD13152c	1	80	5,9	No	Classic	2,7	0	Positive	Negative	Negative	25	2	5

PD9860g	1	47	10,4	Yes	Classic	4,2	16	Positive		Negative	2	2	14
PD9879c	1	87	13,3	No	Classic	3,2	0	Negative	Negative	Positive	10	2	10
PD9880c	1	63	1,1	Yes	Classic	4,9	2	Positive	Positive	Negative	24	2	2
PD13155a	1	75	8,6	No	Trabecular	1,5	0	Positive	Positive	Negative	67,5	2	3
PD13156a	1	72	11	Yes	Classic	3	1	Positive	Positive	Negative	18	2	8
PD9881d	1	68	15,3	No	Mixed, non classic	1,5	0	Positive	Positive	Negative	15	2	9
PD9905c	1	79	1,3	Yes	Alveolar	2		Positive	Positive	Negative	21	2	2
PD13157a	1	70	10,6	No	Solid	2,8	1	Positive	Positive	Negative	6	2	7
PD9909f	1	51	8,2	Yes	Classic	3,5	15	Positive	Positive	Negative	5	2	12
PD13158a	1	52	2	Yes	Classic	2,2	8	Negative	Negative	Positive	10	2	20
PD13824a	4	53	12,2	No	Mixed, non classic	5,5	2	Positive	Positive	Negative	12	2	6
PD13832a	4	42	2,6	Yes	Solid	2	1	Positive	Positive	Negative	10	2	6
PD13896a	4	54	15,1	Yes	Classic	1,3	14	Positive	Positive	Negative	15	2	8
PD13897a	4	71	14,5	No	Classic	0,8		Positive	Negative	Negative	25	2	5
PD13898a	4	43	9,2	No	Alveolar	1,5	0	Positive	Positive	Negative	40	2	6
PD13899a	4	46	16,6	No	Mixed, non classic	1,5	0	Positive	Positive	Negative	9	3	6
PD13900a	4	55	11,6	No	Mixed, non classic	1,5	0	Positive	Positive	Negative	24	3	7
PD13901a	4	48	6,5	No	Classic	2,7	6	Positive	Positive	Negative	17	2	3
PD13902a	4	79	3,2	Yes	Alveolar	2	23	Positive	Positive	Negative	40	3	10
PD13903a	4	71	9	No	Alveolar	1,4	0	Positive	Negative	Negative	22	2	2
PD13904a	4	46	16,4	No	Alveolar	1,1	2	Positive	Positive	Negative	15	2	15
PD13905a	4	49	13,5	No	Alveolar	1,5	3	Positive	Positive	Negative	18	2	9
PD13906a	4	54	3,8	Yes	Classic	1,7	0	Positive	Negative	Negative	23	2	5
PD13907a	4	56	10,4	Yes	Classic	5,5	3	Positive	Negative	Negative	9	2	7
PD13908a	4	56	11,9	No	Classic	0,8	0	Negative	Negative	Negative	3	2	4
PD13910a	4	44	14,9	No	Mixed, non classic	1,5	1	Positive	Positive	Negative	32	2	7
PD13911a	4	50	12	No	Solid	2	0	Positive	Positive	Negative	18	3	17
PD13833a	4	67	14,4	No	Classic	1,5	0	Positive	Negative	Negative	4	2	20
PD13912a	4	56	14	No	Classic	2,5	6	Positive	Negative	Negative	2	2	10
PD13913a	4	48	9,9	Yes	Classic	6	10	Positive	Positive	Negative	5	2	6
PD13914a	4	71	9	No	Classic	2,2	0	Positive	Positive	Negative	8	2	2
PD13915a	4	61	12,5	No	Classic	1	0	Positive	Negative	Negative	25	2	3
PD13916a	4	45	12,3	No	Alveolar	1,2		Negative	Positive	Negative	5	1	9
PD13917a	4	83	3,5	No	Classic	2	15	Negative	Negative	Negative	7	2	3
PD13918a	4	73	6,8	Yes	Solid	5,5	18	Positive	Positive	Negative	30	2	2
PD13834a	4	50	11	Yes	Alveolar	1,7	0	Positive	Positive	Negative	30	2	2
PD13919a	4	72	11,9	No	Solid	1,3	1	Positive	Positive	Negative	16	2	3
PD13920a	4	63	12,3	No	Classic	1	0	Positive	Positive	Negative	18	2	4
PD13922a	4	70	5,2	No	Classic	3,5	1	Positive	Positive	Negative	10	2	4
PD13923a	4	37	4,7	Yes	Classic	2,1	2	Negative	Positive	Positive	29	2	2
PD13924a	4	67	14	No	Classic	1,5	0	Positive	Negative	Negative	20	2	3
PD13835a	4	49	17,1	No	Alveolar	1,2	1	Positive	Positive	Negative	20	2	6
PD13925a	4	46	16	No	Classic	1,6	0	Positive	Positive	Negative	22	2	6
PD13926a	4	72	4,5	Yes	Classic	1,2	8	Positive	Positive	Negative	8	2	4

PD13927a	4	56	13	No	Classic	0,6	3	Positive	Positive	Negative	3	1	16
PD13928a2	4	62	12,2	No	Classic	3,5	0	Positive	Positive	Negative	5	2	5
PD13929a	4	68	10,9	No	Classic	5	0	Positive	Negative	Negative	5	2	6
PD13930a	4	69	8,4	No	Alveolar	1,7	0	Positive	Positive	Negative	18	2	3
PD13837a	4	69	14,3	No	Classic	1,9	3	Positive	Negative	Negative	16	2	2
PD13931a	4	49	11,5	No	Mixed, non classic	1,5	0	Positive	Positive	Negative	25	2	7
PD13933a	4	60	8,2	Yes	Alveolar	3,5	15	Positive	Positive	Negative	11	2	1
PD13934a	4	60	11,9	No	Classic	1,5	1	Positive	Positive	Negative	9	2	1
PD13935a	4	48	8,7	Yes	Mixed, non classic	6	24	Positive	Positive	Negative	7	2	8
PD13936a	4	60	15,6	Yes	Alveolar	1,4	0	Positive	Positive	Negative	11	1	6
PD13937a	4	43	12,8	Yes	Alveolar	1	1	Positive	Positive	Negative	4	1	2
PD13838a	4	49	7,2	Yes	Classic	7	25	Positive	Positive	Negative	15	2	3
PD13938a	4	59	1,7	Yes	Classic	5	12	Positive	Positive	Negative	8	2	7
PD13939a	4	74	3,2	Yes	Classic	2,8	0	Positive	Negative	Negative	22	2	1
PD13940a	4	64	10,1	No	Alveolar	0,3		Positive	Positive	Negative	16	2	8
PD13941a	4	42	13,1	No	Alveolar	1,9	4	Positive	Positive	Negative	28	2	6
PD13942a	4	72	0,7	Yes	Alveolar	4	2	Positive	Positive	Negative	3	2	1
PD13943a	4	43	12,5	No	Classic	5	7	Positive	Positive	Negative	15	1	20
PD13944a	4	80	0,5	Yes	Solid	3,4	26	Negative	Negative	Negative	40	3	8
PD13945a	4	86	8,4	Yes	Alveolar	1,6		Positive	Negative	Negative	22	2	3
PD13839a	4	51	15	Yes	Classic	1,2		Positive	Negative	Negative	2	2	5
PD13946a	4	54	2,1	Yes	Alveolar	6,5	16	Positive	Positive	Negative	11	2	5
PD13947a	4	57	6,1	Yes	Classic	1,3	0	Positive	Positive	Negative	16	2	2
PD13948a	4	49	11,9	No	Classic	6,5	6	Positive	Positive	Negative	4	2	7
PD13949a	4	56	7,2	Yes	Mixed, non classic	2,2	0	Positive	Positive	Negative	21	3	8
PD13950a	4	69	9,1	No	Alveolar	2,5	0	Positive	Negative	Negative	8	1	2
PD13951a	4	57	11,6	No	Alveolar	1,4	0	Positive	Negative	Negative	7	2	5
PD13952a	4	53	12,8	No	Mixed, non classic	1,2	0	Positive	Positive	Negative	4	1	11
PD13953a	4	62	8,9	Yes	Classic	2,9	0	Positive	Positive	Negative	9	1	3
PD13954a	4	43	11,2	No	Mixed, non classic	3	1	Positive	Positive	Negative	12	2	5
PD13955a	4	40	11,6	Yes	Mixed, non classic	6	4	Positive	Positive	Negative	20	3	5
PD13956a	4	39	13,4	Yes	Alveolar	1	1	Positive	Positive	Negative	26	3	3
PD13957a	4	68	12,1	No	Alveolar	3,1	6	Positive	Positive	Positive	35	3	15
PD13958a	4	56	11,9	No	Solid	2,5	1	Positive	Positive	Negative	2	1	2
PD13959a	4	69	11	No	Solid	1,8	0	Negative	Negative	Negative	32	3	6
PD13960a	4	45	14,7	No	Alveolar	1,5	0	Positive	Positive	Negative	10	2	1
PD13825a	4	48	14,2	No	Classic	2,4	0	Positive	Positive	Negative	18	1	5
PD13840a	4	76	13,4	No	Solid	2,6	0	Positive	Positive	Negative	25	2	3
PD13961a	4	66	12,9	No	Solid	3	8	Positive	Positive	Negative	41	3	5
PD13962a	4	50	4	Yes	Alveolar	1,9	0	Positive	Positive	Negative	15	2	3
PD13963a	4	55	9,8	No	Classic	3	0	Positive	Positive	Negative	4	2	14
PD13964a	4	70	2,9	No	Alveolar	1,9	0	Positive	Positive	Negative	12	2	10
PD13965a	4	60	11,4	No	Classic	2,1	0	Positive	Positive	Negative	8	1	1
PD13966a	4	57	12,7	No	Classic	2,4	0	Positive	Positive	Negative	18	2	5

PD13967a	4	55	7,9	No	Classic	2,2	2	Positive	Positive	Negative	6	2	9
PD13968a	4	57	0,3	Yes	Alveolar	2,1	11	Positive	Positive	Negative	14	2	3
PD13841a	4	55	2,1	Yes	Mixed, non classic	1,2	22	Negative	Negative	Negative	60	3	60
PD13969a	4	67	2,4	Yes	Alveolar	1,1	2	Positive	Negative	Negative	15	3	11
PD13970a	4	64	11,5	No	Classic	1,1	0	Positive	Positive	Negative	5	2	3
PD13971a	4	57	11,5	No	Classic	2,5	0	Positive	Negative	Negative	10	2	4
PD13972a	4	58	7,8	No	Solid	4	2	Positive	Positive	Negative	22	3	3
PD13973a	4	78	13,8	No	Alveolar	1,2	0	Positive	Negative	Negative	22	2	2
PD13974a	4	39	9,8	No	Alveolar	2	0	Positive	Positive	Negative	32	3	15
PD13975a	4	48	11,9	No	Alveolar	1,4	0	Positive	Negative	Negative	13	2	3
PD13977a	4	42	10	Yes	Solid	2,1	3	Positive	Positive	Negative	80	3	5
PD13978a	4	51	12,1	Yes	Solid	2,5	0	Positive	Positive	Negative	25	2	5
PD13842a	4	55	15,7	No	Alveolar	4	3	Positive	Positive	Negative	15	2	2
PD13980a	4	50	13,4	No	Mixed, non classic	1,3	0	Positive	Positive	Positive	21	3	15
PD13982a	4	66	12,6	No	Solid	0,8	0	Positive	Positive	Negative	9	1	4
PD13983a	4	47	12,5	No	Mixed, non classic	3	2	Positive	Positive	Negative	45	3	5
PD13984a	4	65	2,2	Yes	Classic	5,5	43	Positive	Positive	Negative	24	2	10
PD13985a	4	52	11,3	No	Alveolar	1,8	1	Positive	Positive	Negative	13	2	10
PD13986a	4	67	9,5	No	Alveolar	1,9	0	Positive	Positive	Negative	14	2	5
PD13987a	4	47	13,1	Yes	Mixed, non classic	3	3	Positive	Positive	Negative	6	2	5
PD13988a	4	67	7,2	Yes	Alveolar	2,5	0	Positive	Positive	Negative	8	3	2
PD13989a	4	40	14,3	No	Classic	4,3	2	Positive	Positive	Negative	20	2	4
PD13990a	4	51	12,2	No	Mixed, non classic	1,5	2	Positive	Positive	Negative	12	2	2
PD13991a	4	39	13,8	No	Alveolar	1	0	Positive	Positive	Negative	17	2	5
PD13992a	4	60	4,7	No	Classic	2,3	1	Positive	Positive	Negative	3	2	4
PD13843a	4	57	16	Yes	Classic	4,5	4	Positive	Positive	Negative	6	2	5
PD13993a	4	62	4,2	Yes	Solid	1,5	1	Positive	Positive	Negative	17	2	5
PD13994a	4	49	10,7	No	Classic	2,5	0	Positive	Positive	Negative	13	2	3
PD13996a	4	46	11,1	No	Classic	3,5	2	Positive	Positive	Negative	25	2	2
PD13997a	4	50	13,5	No	Classic	1,1	0	Positive	Positive	Negative	10	2	2
PD13998a	4	66	10,5	No	Classic	4,5	3	Positive	Positive	Negative	20	2	10
PD13999a	4	44	3,3	Yes	Mixed, non classic	3	2	Positive	Positive	Negative	10	2	40
PD14000a	4	44	11,1	No	Solid	1,6	0	Positive	Positive	Negative	30	2	11
PD14001a	4	62	6	No	Mixed, non classic	1,2	17	Negative	Negative	Positive	35	3	30
PD14002a	4	69	3,7	Yes	Solid	1,5	0	Positive	Positive	Negative	25	2	3
PD13844a	4	48	14,7	No	Classic	0,9		Positive	Negative	Negative	6	2	5
PD14003a	4	52	10,7	No	Classic	0,7	3	Positive	Positive	Negative	16	2	1
PD14004a	4	47	12,8	No	Alveolar	1	0	Positive	Positive	Negative	15	2	2
PD14005a	4	69	11	Yes	Alveolar	1,7	3	Positive	Positive	Negative	15	2	10
PD14006a	4	50	13,7	No	Mixed, non classic	7	9	Positive	Positive	Negative	19	2	4
PD14007a	4	58	10,8	No	Alveolar	2,3	2	Positive	Negative	Negative	10	2	4
PD13845a	4	52	10,7	No	Solid	1,3	0	Positive	Positive	Negative	20	2	22
PD14008a	4	54	12,5	No	Solid	10	4	Positive	Positive	Negative	25	2	25
PD14009a	4	50	12,7	No	Classic	1,2	0	Positive	Positive	Negative	22	2	6

PD14010a	4	47	6,9	Yes	Mixed, non classic	1,4	5	Positive	Positive	Negative	19	1	7
PD14011a	4	64	12	No	Classic	2,7	0	Positive	Negative	Negative	16	1	2
PD14012a	4	64	10,8	No	Alveolar	1,5	5	Positive	Positive	Negative	13	3	5
PD14013a	4	40	12,1	No	Solid	1,8	12	Positive	Positive	Negative	19	2	4
PD14014a	4	39	9,1	No	Alveolar	1,5	0	Positive	Positive	Negative	48	3	5
PD14016a	4	64	7,5	Yes	Classic	6,7	0	Positive	Negative	Negative	15	2	3
PD14017a	4	35	6	Yes	Classic	3,5	3	Positive	Negative	Negative	28	2	6
PD14018a	4	48	11,2	No	Classic	4	1	Positive	Negative	Negative	3	1	3
PD14019a	4	49	12,1	No	Alveolar	1,2	0	Positive	Positive	Negative	8	2	3
PD14020a	4	58	12,6	No	Classic	2,5	0	Positive	Positive	Negative	4	1	1
PD14021a	4	47	10,2	No	Alveolar	3	10	Positive	Positive	Negative	12	2	1
PD14022a	4	60	8,8	Yes	Classic	1,7	2	Positive	Negative	Negative	3	1	3
PD14023a	4	67	2,5	Yes	Classic	8	8	Positive	Positive	Negative	19	2	2
PD14024a	4	81	6,8	No	Classic	2,4		Positive	Positive	Negative	14	1	3
PD14025a	4	56	8,9	Yes	Solid	1,9	0	Positive	Positive	Negative	17	1	3
PD14026a	4	39	11,3	No	Classic	6,5	0	Positive	Positive	Negative	7	2	2
PD14027a	4	38	11	No	Classic	3,2	1	Positive	Positive	Negative	11	2	5
PD13846a	4	41	12,3	No	Mixed, non classic	1	0	Positive	Negative	Negative	12	2	6
PD14028a	4	58	10,5	No	Classic	1	0	Positive	Positive	Negative	21	2	2
PD14029a	4	47	10,3	No	Classic	4	0	Positive	Positive	Negative	16	2	3
PD14030a	4	43	7,6	Yes	Classic	1,4	0	Positive	Positive	Negative	22	2	4
PD14031a	4	69	9,4	Yes	Alveolar	1,5	2	Positive	Positive	Negative	8	2	2
PD14032a	4	71	8	No	Classic	1,5	2	Positive	Positive	Negative	15	2	3
PD13826a	4	60	0,7	No	Solid	2	1	Positive	Positive	Negative	18	2	3
PD13847a	4	61	10,6	No	Classic	1,2	0	Positive	Positive	Negative	2	1	5
PD14033a	4	44	10,7	No	Classic	11	2	Positive	Positive	Negative	8	2	4
PD14034a	4	41	6,3	Yes	Classic	2,3	0	Positive	Positive	Negative	8	2	5
PD14035a	4	55	12,3	No	Solid	2,4	0	Positive	Positive	Negative	24	2	4
PD14036a	4	50	10,9	No	Classic	1,4	2	Positive	Positive	Negative	30	2	4
PD14037a2	4	59	12,4	Yes	Classic	0,7	0	Positive	Positive	Negative	31	2	3
PD14038a	4	62	9,9	No	Mixed, non classic	4,8	13	Positive	Negative	Negative	10	2	4
PD14039a2	4	36	12,7	No	Mixed, non classic	2,5	6	Positive	Positive	Positive	38	3	5
PD14040a	4	52	3,3	Yes	Alveolar	1,5	1	Positive	Positive	Negative	16	2	3
PD14041a	4	39	11,8	No	Classic	0,7	0	Positive	Positive	Positive	15	2	4
PD14042a	4	67	5	Yes	Alveolar	5,7	0	Positive	Positive	Negative	12	3	4
PD14044a	4	75	9,9	No	Classic	4	3	Positive	Positive	Negative	14	2	5
PD14045a	4	45	10,9	No	Classic	1,5	3	Positive	Positive	Negative	9	2	5
PD14046a	4	46	11,4	No	Solid	2,1	0	Positive	Positive	Negative	26	2	2
PD14047a2	4	64	13,3	No	Mixed, non classic	5,1	0	Positive	Positive	Negative	17	2	3
PD14048a	4	61	14,1	Yes	Alveolar	2,8	1	Positive	Positive	Negative	12	2	8
PD13848a	4	31	15,2	No	Classic	1,4	0	Positive	Positive	Negative	5	2	2
PD14049a	4	45	9,6	Yes	Classic	2,4	0	Positive	Positive	Negative	35	2	5
PD14050a2	4	59	9,7	No	Solid	6	0	Positive	Positive	Negative	24	2	1
PD14051a	4	48	12,7	No	Mixed, non classic	2,5	3	Positive	Positive	Negative	5	2	3

PD14052a	4	70	6,4	No	Classic	4	0	Positive	Positive	Negative	24	2	5
PD14053a	4	55	9,6	No	Classic	5,2	0	Positive	Positive	Negative	12	2	4
PD14054a	4	41	10,4	No	Solid	1,1	2	Positive	Positive	Negative	11	2	5
PD14055a2	4	75	10,3	No	Classic	1,8	1	Positive	Positive	Negative	22	2	7
PD13849a	4	59	13,3	No	Alveolar	0,6		Positive	Negative	Negative	2	1	2
PD14056a	4	65	7	No	Alveolar	2,1	29	Positive	Positive	Negative	12	2	3
PD14057a	4	58	10,6	No	Classic	1,5	1	Positive	Positive	Negative	4	2	6
PD14058a	4	61	6,8	No	Classic	1,6	0	Positive	Positive	Negative	13	2	5
PD14059a	4	75	0,4	Yes	Alveolar	3	23	Positive	Negative	Negative	15	2	3
PD14060a	4	57	4,9	Yes	Mixed, non classic	1,3	1	Positive	Positive	Positive	27	3	10
PD14061a	4	78	13,6	No	Classic	1,5	0	Positive	Positive	Negative	8	2	2
PD14062a	4	48	10,3	No	Alveolar	3,6	0	Positive	Positive	Negative	24	2	4
PD14063a	4	48	10,5	No	Classic	2,3	0	Positive	Positive	Negative	11	2	6
PD14064a	4	68	3,9	Yes	Classic	1,1	2	Positive	Negative	Negative	8	2	25
PD13850a	4	47	14,3	No	Classic	3	2	Positive	Positive	Negative	8	2	20
PD14065a	4	50	10,3	No	Classic	7	16	Positive	Positive	Negative	8	2	3
PD14066a	4	84	9,6	No	Solid	1,6	0	Positive	Negative	Negative	26	2	6
PD14067a	4	53	9,3	Yes	Alveolar	1,1	4	Negative	Negative	Negative	12	2	25
PD14068a	4	48	3,9	Yes	Mixed, non classic	3,2	6	Positive	Positive	Negative	14	2	10
PD14069a2	4	46	9,3	Yes	Solid	9	10	Positive	Positive	Negative	15	2	5
PD13852a	4	46	14,6	No	Classic	1,8	14	Positive	Positive	Negative	5	2	3
PD13853a	4	54	3,1	Yes	Classic	2,2	0	Positive	Positive	Negative	8	1	7
PD13854a	4	74	7,2	No	Alveolar	4,5	9	Positive	Positive	Negative	12	2	7
PD13855a	4	56	9,2	Yes	Alveolar	0,8		Positive	Negative	Negative	10	2	3
PD14071a2	4	75	12,1	No	Classic	2,8	0	Positive	Positive	Negative	10	2	1
PD13827a	4	57	15,6	No	Classic	1,3	0	Positive	Positive	Negative	3	2	5
PD13856a	4	55	5,6	Yes	Alveolar	4	0	Positive	Positive	Negative	8	2	5
PD14072a	4	79	3,8	Yes	Solid	3,4	3	Positive	Positive	Positive	6	2	1
PD14073a	4	80	12,1	No	Classic	2,2	0	Positive	Negative	Negative	15	2	8
PD14074a	4	53	5,4	Yes	Solid	2,2	0	Positive	Positive	Negative	25	3	3
PD14075a	4	54	10,3	No	Alveolar	1,4	0	Positive	Negative	Negative	11	2	21
PD14076a	4	67	12	No	Solid	2,2	0	Positive	Positive	Negative	22	2	20
PD13857a	4	64	7,9	Yes	Solid	1,7	0	Positive	Negative	Negative	13	2	6
PD14077a	4	45	2,7	No	Classic	4,5	23	Positive	Positive	Negative	12	2	4
PD13858a	4	64	17,2	No	Solid	1,5	0	Positive	Positive	Negative	10	2	5
PD14078a	4	49	10,8	No	Classic	1,2	0	Positive	Positive	Positive	10	3	6
PD14079a	4	62	11,3	No	Solid	1,3	1	Positive	Positive	Negative	27	2	6
PD14080a	4	57	7,3	No	Solid	2	0	Positive	Positive	Negative	29	2	2
PD14081a	4	51	10,1	No	Classic	4,5	0	Positive	Positive	Negative	5	2	5
PD13859a	4	47	1,4	Yes	Alveolar	1	0	Positive	Positive	Negative	10	2	10
PD14082a	4	47	8,4	No	Mixed, non classic	3,5	10	Positive	Positive	Negative	18	3	5
PD14083a	4	42	8,5	No	Alveolar	2,8	1	Positive	Positive	Negative	16	2	2
PD14084a	4	44	9,9	No	Classic	1,8	28	Positive	Positive	Negative	13	2	6
PD14085a	4	56	5,8	No	Mixed, non classic	2,5	0	Positive	Positive	Negative	18	2	1

PD13860a	4	38	2,2	Yes	Solid	2,1	3	Negative	Positive	Negative	18	2	4
PD14086a	4	37	5,2	No	Alveolar	3,5	2	Positive	Positive	Negative	8	2	3
PD14087a	4	67	3,8	Yes	Mixed, non classic	2,2	25	Positive	Positive	Negative	18	3	19
PD14088a	4	49	12,4	No	Alveolar	3	0	Positive	Positive	Negative	25	3	4
PD14089a	4	65	4,5	No	Solid	6	1	Positive	Negative	Negative	13	2	3
PD14090a	4	38	12,2	No	Classic	1,9	0	Positive	Negative	Negative	10	2	1
PD13861a	4	52	9,9	No	Mixed, non classic	1	15	Positive	Negative	Negative	2	1	2
PD13862a	4	74	0,4	Yes	Alveolar	1,5		Positive	Positive	Negative	18	2	2
PD13863a	4	54	12,4	Yes	Alveolar	1,3		Positive	Positive	Negative	3	1	2
PD14092a	4	37	8,1	Yes	Mixed, non classic	7,5	7	Positive	Positive	Negative	26	2	11
PD14093a	4	49	5,7	Yes	Solid	1,5	0	Positive	Positive	Negative	40	3	5
PD14094a	4	64	4,5	Yes	Mixed, non classic	4,8	6	Positive	Negative	Positive	35	3	4
PD14095a	4	61	10	No	Classic	1,5	0	Positive	Positive	Negative	15	2	5
PD14096a	4	70	11,3	No	Classic	1,5	0	Positive	Negative	Negative	10	2	2
PD13864a	4	60	5,3	Yes	Alveolar	2,3	0	Positive	Positive	Negative	7	2	3
PD14097a	4	48	9,8	No	Classic	2,2	0	Positive	Negative	Negative	7	1	5
PD14098a	4	40	11,3	No	Mixed, non classic	4	0	Positive	Positive	Negative	25	2	5
PD14099a	4	40	0,2	Yes	Mixed, non classic	4,2	33	Negative	Negative	Positive	24	3	5
PD14100a	4	53	8,5	No	Alveolar	0,9	0	Positive	Positive	Negative	10	1	4
PD14101a	4	49	8,8	No	Classic	1,7	1	Positive	Positive	Negative	12	3	6
PD14102a	4	66	8,9	No	Classic	2,7	8	Positive	Positive	Negative	23	2	3
PD13828a	4	69	11,3	No	Solid	1,5	0	Positive	Positive	Negative	5	2	4
PD13865a	4	47	13,4	No	Alveolar	0,5		Positive	Negative	Negative	4	2	1
PD14103a	4	50	7,5	No	Classic	1,1	1	Positive	Positive	Negative	10	2	4
PD14104a	4	55	9,4	No	Classic	2,2	0	Positive	Positive	Positive	11	2	2
PD14105a2	4	64	9,3	No	Solid	1,7	0	Positive	Positive	Negative	21	1	4
PD14106a	4	56	2,5	Yes	Classic	4,3	2	Positive	Positive	Negative	12	2	6
PD13866a	4	59	8,3	No	Alveolar	7	0	Positive	Positive	Negative	6	2	5
PD14107a	4	75	4,6	No	Solid	5,5	58	Positive	Positive	Negative	40	3	14
PD14108a	4	63	10	No	Classic	1,2	0	Positive	Positive	Negative	21	2	20
PD14109a	4	54	11,4	Yes	Solid	2,5	17	Positive	Positive	Negative	35	3	4
PD14110a	4	61	7,6	No	Alveolar	4,7	18	Positive	Positive	Negative	13	2	3
PD14111a	4	63	8,5	No	Alveolar	1,5	4	Positive	Positive	Negative	27	3	1
PD14112a	4	61	10,7	No	Mixed, non classic	2	0	Positive	Positive	Negative	37	3	2
PD14113a	4	41	10	No	Alveolar	1,6	0	Positive	Positive	Negative	18	2	13
PD14114a	4	69	10,3	No	Solid	4,5	0	Positive	Positive	Negative	12	2	5
PD14115a	4	71	9,9	No	Alveolar	1	1	Positive	Positive	Negative	45	3	3
PD14116a	4	70	7,9	No	Classic	1,5	0	Positive	Negative	Negative	9	2	1
PD13867a	4	60	13,5	No	Classic	1,9	1	Positive	Positive	Negative	9	2	4
PD14117a	4	56	9,5	No	Classic	0,8	0	Positive	Positive	Negative	17	1	2
PD14118a2	4	48	11,8	No	Classic	2,5	2	Positive	Positive	Negative	19	2	3
PD14119a	4	87	3,5	No	Classic	4,5	21	Positive	Positive	Positive	16	2	4
PD14120a	4	34	3,5	Yes	Classic	4	0	Positive	Positive	Negative	18	2	1
PD14121a	4	53	4,5	No	Mixed, non classic	2,4	3	Positive	Positive	Negative	22	3	2

PD14122a	4	44	9,9	No	Mixed, non classic	1,8	0	Positive	Positive	Negative	13	2	4
PD14123a	4	56	9,9	No	Classic	2,4	0	Positive	Positive	Negative	12	2	6
PD14124a	4	53	1,4	Yes	Classic	1,2	1	Positive	Positive	Negative	22	2	12
PD14125a	4	56	9,6	No	Classic	1,1	13	Positive	Negative	Negative	11	2	3
PD14126a	4	42	7,7	No	Classic	4,5	3	Positive	Positive	Negative	17	2	5
PD14127a	4	42	8,9	Yes	Classic	2,4	2	Positive	Positive	Negative	17	2	11
PD13868a	4	49	13,6	No	Classic	1	0	Positive	Positive	Negative	5	2	4
PD14128a	4	50	8,6	No	Classic	2,6	3	Positive	Negative	Negative	20	2	5
PD14129a	4	65	7,8	No	Classic	1,8	2	Positive	Positive	Negative		2	25
PD14130a	4	32	9,6	No	Mixed, non classic	1,4	4	Positive	Positive	Negative	42	3	2
PD14132a	4	64	11,4	Yes	Alveolar	1,9	0	Positive	Positive	Negative	12	2	2
PD14133a	4	37	7,6	No	Alveolar	1,5	6	Positive	Positive	Negative	31	2	7
PD14134a	4	67	10,4	No	Alveolar	1,5	2	Positive	Positive	Negative	16	2	4
PD14135a	4	47	8,8	No	Mixed, non classic	2,5	1	Negative	Negative	Negative	40	3	25
PD13869a	4	47	14,2	Yes	Classic	1,5	0	Negative	Positive	Negative	22	3	4
PD14136a	4	44	10,3	No	Classic	1,1	0	Positive	Positive	Negative	15	2	3
PD14137a	4	48	2,2	Yes	Solid	1,8	27	Negative	Negative	Negative	36	3	35
PD14138a	4	41	10,7	Yes	Classic	2,7	2	Positive	Positive	Negative	24	2	14
PD14139a	4	50	9,7	No	Alveolar	1,2	0	Positive	Positive	Negative	12	2	3
PD14140a	4	36	9,5	No	Classic	3	1	Positive	Positive	Negative	8	1	3
PD14141a	4	66	6,1	No	Classic	1,4	0	Positive	Positive	Negative	12	2	3
PD14142a	4	34	8,1	No	Classic	2,8	0	Positive	Positive	Negative	12	2	15
PD13870a	4	73	9,1	Yes	Classic	2,5	10	Positive	Positive	Negative	9	2	3
PD14143a	4	51	9,5	No	Classic	2,2	0	Positive	Positive	Negative	37	2	14
PD14144a	4	64	3,2	Yes	Classic	1,2	0	Positive	Positive	Negative	10	2	4
PD14145a	4	67	5,9	No	Mixed, non classic	2,1	0	Positive	Negative	Negative	18	2	30
PD14146a	4	78	10,6	No	Classic	1,5	0	Positive	Negative	Negative	5	2	8
PD14147a	4	65	10,1	No	Classic	1,2	0	Positive	Positive	Negative	9	1	3
PD14148a	4	60	8,9	No	Alveolar	4	0	Positive	Positive	Negative	19	2	2
PD14149a	4	57	9,2	No	Alveolar	1,3	0	Positive	Negative	Negative	4	1	1
PD14150a	4	49	9,3	No	Classic	3,2	0	Positive	Negative	Negative	9	1	7
PD13871a	4	47	9,7	No	Mixed, non classic	1,5	1	Positive	Positive	Negative	12	3	12
PD14151a	4	45	6	Yes	Mixed, non classic	5,5	12	Positive	Positive	Negative	23	2	17
PD14152a	4	54	9,9	No	Alveolar	1,8	0	Positive	Positive	Positive	12	2	3
PD13829a	4	55	4	Yes	Mixed, non classic	4	9	Positive	Positive	Negative	20	3	4
PD14153a	4	42	4,6	Yes	Mixed, non classic	1,8	0	Positive	Positive	Negative	20	2	6
PD14154a	4	64	8,7	No	Classic	1	0	Positive	Positive	Negative	15	2	3
PD14155a	4	71	10,9	No	Solid	1,5	0	Positive	Positive	Negative	16	2	10
PD14156a	4	37	10,6	No	Classic	5,6	1	Positive	Positive	Negative	11	2	7
PD14157a	4	59	3,9	Yes	Solid	4,6	3	Positive	Negative	Negative	38	2	3
PD13872a	4	50	5,7	No	Solid	3	2	Positive	Negative	Negative	22	2	5
PD14158a	4	59	9,9	No	Solid	1,1	1	Positive	Positive	Negative	26	2	5
PD14159a	4	64	8,8	No	Classic	1,4	0	Positive	Positive	Negative	15	2	4
PD14160a	4	81	1	No	Alveolar	4,8	9	Positive	Negative	Negative	20	2	10

PD13873a	4	39	11,7	No	Classic	3,5	1	Positive	Positive	Negative	15	2	35
PD14162a	4	56	9,8	No	Mixed, non classic	2,2	1	Positive	Positive	Negative	25	2	25
PD14163a	4	48	10,4	No	Classic	1	0	Positive	Positive	Negative	24	2	4
PD14164a	4	48	8,2	No	Classic	1,9	0	Positive	Positive	Negative	27	2	6
PD14165a	4	60	8,9	No	Classic	1,3	0	Positive	Positive	Negative	11	2	5
PD14166a	4	55	1,4	Yes	Solid	2,7	8	Positive	Positive	Negative	28	2	20
PD14167a	4	66	8,1	No	Classic	2,2	23	Positive	Negative	Negative	12	2	2
PD14168a	4	47	3,3	Yes	Mixed, non classic	2,2	25	Positive	Positive	Negative	52	3	40
PD14169a	4	48	6,8	No	Mixed, non classic	2	8	Positive	Positive	Negative	19	2	3
PD14170a2	4	48	9,4	No	Classic	2	0	Positive	Positive	Negative	27	2	3
PD14171a	4	47	9,6	No	Mixed, non classic	2,3	3	Negative	Negative	Positive	47	3	20
PD14172a	4	65	8,2	No	Classic	2,7	7	Positive	Positive	Negative	13	2	5
PD14173a	4	53	9,4	No	Classic	2,9	0	Positive	Positive	Negative	6	1	2
PD14174a	4	45	10,2	No	Mixed, non classic	1,5	0	Positive	Positive	Negative	40	3	10
PD14175a	4	46	6,9	No	Alveolar	1	0	Positive	Positive	Negative	21	2	6
PD14176a	4	45	6,5	No	Solid	3	3	Positive	Positive	Negative	10		4
PD14177a	4	42	9	No	Classic	5,5	2	Positive	Positive	Negative	18	3	4
PD14178a	4	69	8,7	No	Trabecular	1,2	0	Positive	Positive	Negative	14	2	2
PD14179a	4	73	2,8	Yes	Mixed, non classic	6	23	Positive	Positive	Negative	14	2	11
PD14180a	4	42	9,9	No	Classic	7,5	4	Positive	Positive	Negative	12	2	6
PD14181a	4	63	8,2	No	Classic	1,8	0	Positive	Negative	Negative	11	1	2
PD14182a	4	49	9,1	No	Solid	4,5	0	Positive	Negative	Negative	21	2	20
PD14183a	4	76	2,1	Yes	Classic	3,1		Positive	Positive	Negative	25	2	1
PD13874a	4	86	0,5	Yes	Solid	3,5	5	Positive	Positive	Negative	27	2	1
PD14184a	4	81	10,4	No	Alveolar	1,9	0	Positive	Positive	Negative	12	1	1
PD14185a	4	46	8	No	Classic	2,4	0	Positive	Positive	Negative	7	1	3
PD14186a	4	73	10	No	Solid	1,4	0	Positive	Positive	Negative	33	2	2
PD14187a	4	45	9,2	No	Mixed, non classic	5	36	Positive	Positive	Negative	37	2	7
PD13875a	4	54	16,5	Yes	Classic	2,2	0	Positive	Positive	Negative	23	3	4
PD14188a	4	52	7,8	No	Mixed, non classic	2	0	Positive	Negative	Negative	12	2	5
PD14189a	4	62	1,7	Yes	Mixed, non classic	5	19	Positive	Positive	Negative	11	2	2
PD14190a	4	46	9	No	Mixed, non classic	1,7	1	Positive	Positive	Negative	15	2	4
PD14191a	4	83	5,9	No	Classic	3,9	0	Positive	Positive	Negative	11		1
PD14192a2	4	56	8,6	No	Solid	4,3	2	Positive	Positive	Negative	12	2	3
PD14193a	4	39	9,8	No	Solid	1,1	0	Positive	Positive	Negative	43	2	10
PD14194a	4	38	5,1	No	Solid	6,5	3	Positive	Positive	Negative	28	2	3
PD14195a	4	67	7	No	Classic	2,1	3	Positive	Positive	Negative	11	2	4
PD14196a	4	40	9,6	No	Solid	5,1	11	Positive	Positive	Negative	21	2	20
PD13876a	4	40	8,3	No	Mixed, non classic	7,5	1	Positive	Positive	Negative	10	2	6
PD14197a	4	58	7,6	No	Trabecular	0,6	0	Positive	Positive	Negative	18	2	2
PD14198a	4	70	1,3	Yes	Solid	2,1	0	Positive	Negative	Negative	25	2	3
PD14199a	4	50	8,9	No	Alveolar	3,9	0	Positive	Positive	Negative	12	2	4
PD14200a	4	45	9,5	No	Mixed, non classic	1,9	0	Positive	Positive	Negative	24	3	5
PD14201a	4	83	5,9	No	Alveolar	3,5		Positive	Positive	Negative	10	1	1

PD13877a	4	65	5	No	Solid	3,4	7	Positive	Positive	Negative	22	3	4
PD14202a	4	40	6,8	Yes	Trabecular	2,1	10	Positive	Positive	Negative	23	2	5
PD14203a	4	40	6,4	No	Trabecular	7	7	Positive	Negative	Negative	16	2	6
PD13878a	4	42	9,5	No	Mixed, non classic	1,8	0	Positive	Positive	Negative	18	3	9
PD13879a	4	67	4,2	No	Solid	4	0	Positive	Negative	Negative	40	3	3
PD14204a	4	76	9,2	No	Classic	3,8	1	Positive	Positive	Negative	19	2	8
PD14205a	4	47	7,5	No	Classic	2,5	0	Positive	Positive	Negative	5	1	3
PD14206a	4	51	6,1	No	Classic	1,5	5	Positive	Positive	Negative	6	2	4
PD14207a	4	66	6,1	No	Alveolar	2,1	1	Positive	Positive	Negative	10	3	7
PD14209a	4	52	1,4	Yes	Solid	3	2	Positive	Positive	Positive	25	3	5
PD14210a	4	45	7,1	No	Alveolar	1,1	0	Positive	Positive	Negative	14	2	4
PD14211a	4	62	5,5	No	Mixed, non classic	2,1	0	Positive	Positive	Negative	28		4
PD14212a	4	40	8,5	No	Trabecular	1,3	0	Positive	Positive	Negative	7	1	3
PD14213a	4	45	6,8	No	Classic	1,5	2	Positive	Positive	Negative	22	2	4
PD14214a	4	46	5,7	No	Classic	2,3	2	Positive	Positive	Negative	5	2	5
PD14215a	4	55	6,5	Yes	Classic	1,6	13	Positive	Negative	Negative	10	2	3
PD14217a	4	53	7,2	No	Classic	0,8	0	Positive	Positive	Negative	13	1	4
PD14218a	4	60	6,4	No	Alveolar	1,8	1	Positive	Negative	Negative	27	2	3
PD14219a	4	57	7	No	Classic	1,5	2	Positive	Positive	Negative	23	2	6
PD14220a	4	56	6,1	No	Classic	1,6	1	Positive	Negative	Negative	9	2	5
PD14221a	4	71	2	No	Classic	0,8	0	Positive	Positive	Negative	9	2	3
PD14222a	4	48	8,8	No	Mixed, non classic	2,2	2	Positive	Positive	Negative	12	2	8
PD13880a	4	45	11,4	No	Alveolar	1,4	1	Positive	Positive	Negative	7	3	7
PD14223a	4	73	9,2	No	Alveolar	2,2	0	Positive	Positive	Negative	15	1	2
PD14224a	4	50	8,6	Yes	Solid	3,8	33	Positive	Positive	Negative	32	3	9
PD14225a	4	47	6,7	No	Trabecular	1,1	1	Positive	Positive	Negative	29	2	6
PD14226a	4	55	7,4	No	Mixed, non classic	4	0	Positive	Positive	Negative	10	2	3
PD13830a	4	29	2,8	Yes	Mixed, non classic	3	0	Positive	Positive	Negative	32	2	5
PD14227a	4	47	6,3	Yes	Solid	3,8	0	Positive	Positive	Negative	29	3	3
PD14228a	4	54	6,6	No	Classic	1,8	1	Positive	Negative	Negative	3	1	2
PD14230a2	4	37	8,5	No	Classic	3	2	Positive	Positive	Negative	8	1	7
PD14231a	4	76	8,1	No	Alveolar	0,9	0	Positive	Positive	Negative	12	2	2
PD14232a	4	44	8,5	No	Classic	3,5	2	Positive	Positive	Negative	10	2	9
PD13881a	4	39	13,6	No	Classic	1	0	Positive	Positive	Negative	17	2	3
PD14233a	4	44	8,6	No	Classic	4,5	0	Positive	Positive	Negative	6	1	10
PD14234a	4	48	8	No	Alveolar	1,5	1	Positive	Positive	Negative	31	3	5
PD14235a	4	42	8,6	Yes	Alveolar	3,7	3	Positive	Positive	Negative	40	3	7
PD14236a	4	59	3,5	Yes	Classic	7,5	35	Positive	Positive	Negative	18	2	1
PD14237a	4	65	0,3	Yes	Mixed, non classic	8	27	Positive	Negative	Negative	18	2	6
PD14238a	4	67	2,4	Yes	Classic	3		Positive	Negative	Negative	10	2	2
PD13882a	4	59	13,4	No	Classic	3,5	0	Positive	Positive	Negative	10	2	12
PD14239a	4	44	5,6	No	Classic	3,4	1	Positive	Positive	Negative	11	2	4
PD14241a	4	49	4,3	Yes	Mixed, non classic	1,2	0	Positive	Positive	Negative	23	2	6
PD14242a	4	85	8,6	No	Mixed, non classic	1,3		Positive	Positive	Negative	16	2	7

PD13883a	4	58	14,4	No	Solid	2	1	Negative	Positive	Negative	35	3	2
PD14243a	4	49	8	No	Mixed, non classic	4	1	Positive	Positive	Negative	12	2	2
PD14244a	4	50	7,1	No	Alveolar	2,1	0	Positive	Positive	Negative	20		6
PD14245a	4	48	8	No	Alveolar	1,2	0	Positive	Positive	Negative	9	2	5
PD14246a	4	71	7,1	No	Classic	3	5	Positive	Positive	Negative	4	1	1
PD14247a	4	65	7,1	No	Classic	2,4	0	Positive	Positive	Negative	12	2	7
PD14248a	4	42	7,3	Yes	Mixed, non classic	8	1	Positive	Positive	Negative	8	2	7
PD13884a	4	64	13,5	No	Classic	1,5	0	Positive	Positive	Negative	18	2	4
PD14249a	4	61	5,4	No	Classic	3,3	2	Positive	Negative	Negative	3	1	2
PD14250a	4	59	6,4	No	Classic	1,9	0	Positive	Negative	Negative	9	1	2
PD14251a	4	57	5,2	No	Classic	1,4	25	Positive	Positive	Negative	13	2	5
PD14252a	4	71	1,7	Yes	Solid	1,9	0	Positive	Positive	Negative	31	3	2
PD14253a	4	50	6,6	No	Trabecular	4,5	1	Positive	Positive	Negative	14	2	4
PD14254a	4	50	6,1	No	Classic	0,9	1	Positive	Positive	Negative	6	2	5
PD13885a	4	43	5,7	Yes	Classic	1,8	1	Positive	Positive	Negative	22	2	7
PD14256a	4	75	8,7	No	Mixed, non classic	1,4	0	Positive	Positive	Negative	13	3	3
PD14257a	4	44	5,2	No	Mixed, non classic	2,2	3	Positive	Positive	Negative	15	2	6
PD14258a	4	76	4,7	No	Mixed, non classic	4,8	6	Negative	Negative	Negative	17	3	14
PD14259a	4	49	1,1	Yes	Solid	11	14	Negative	Negative	Negative	85	3	7
PD14260a	4	69	6,9	No	Solid	1,4	0	Positive	Positive	Negative	36	3	10
PD14261a	4	69	6,2	No	Classic	4,2	0	Positive	Positive	Negative	9	1	4
PD14262a	4	59	6,8	No	Solid	1,2	0	Positive	Positive	Negative	9	1	2
PD14263a	4	78	4,6	No	Classic	1,4		Positive	Negative	Negative	6	2	14
PD14264a	4	40	8,2	No	Mixed, non classic	2,4	0	Positive	Positive	Negative	19	2	7
PD14265a	4	52	2,5	Yes	Mixed, non classic	2	6	Positive	Positive	Negative	20	1	15
PD13886a	4	48	13,7	No	Alveolar	1,1	0	Positive	Positive	Negative	8	2	5
PD14266a	4	65	7,1	Yes	Solid	1,6		Positive	Positive	Negative	35	3	4
PD14267a	4	70	3,5	No	Classic	5,5	25	Positive	Positive	Negative	8	2	2
PD14268a	4	69	6,4	No	Mixed, non classic	1,7	0	Positive	Negative	Negative	12	2	9
PD14269a	4	51	3,8	Yes	Solid	1,8	3	Positive	Negative	Negative	22	3	2
PD14270a	4	48	7,2	No	Alveolar	3,7	1	Positive	Positive	Negative	18	2	3
PD14271a	4	62	7,7	No	Classic	2,2	0	Positive	Positive	Negative	15	2	5
PD14272a	4	55	6,5	No	Mixed, non classic	0,9	0	Positive	Positive	Negative	26	3	10
PD13887a	4	76	12,7	No	Classic	3,2	0	Positive	Negative	Negative	31	2	6
PD14273a	4	49	2,1	Yes	Alveolar	2,1	1	Positive	Positive	Negative	13	2	2
PD14274a	4	41	8,1	No	Solid	3	0	Positive	Positive	Negative	16	2	10
PD14275a	4	64	6,2	No	Mixed, non classic	1,9	0	Positive	Positive	Negative	12	2	4
PD13831a	4	65	14,3	No	Solid	2,6	0	Positive	Positive	Negative	20	2	5
PD13888a	4	52	12,1	Yes	Mixed, non classic	0,9	2	Positive	Negative	Negative	25	2	6
PD14277a	4	56	5	No	Classic	2,1	1	Positive	Positive	Negative	8	1	3
PD14278a	4	48	5,5	No	Classic	5,2	20	Positive	Positive	Negative	19	2	2
PD14279a	4	77	4,9	No	Classic	1,5	0	Positive	Negative	Negative	7	1	2
PD14280a	4	43	7,6	No	Classic	1,4	0	Positive	Positive	Negative	6	2	2
PD14281a	4	40	6,3	No	Solid	2	0	Positive	Positive	Negative	15		5

PD13889a	4	37	12,5	Yes	Classic	2	0	Positive	Positive	Negative	13	3	2
PD14282a	4	76	7,5	No	Classic	1,5	0	Positive	Positive	Negative	11	2	1
PD14283a	4	47	6,8	No	Trabecular	1,9	2	Positive	Positive	Negative	19	2	2
PD14284a	4	46	6,2	No	Mixed, non classic	4	1	Positive	Positive	Negative	15	3	2
PD14285a	4	69	6,1	No	Solid	2	2	Positive	Positive	Negative	18	3	3
PD13890a2	4	76	11,9	No	Mixed, non classic	3	0	Positive	Positive	Negative	18	2	11
PD14286a	4	55	6,2	No	Alveolar	1,1	0	Positive	Positive	Negative	12	2	2
PD14287a	4	64	1,6	Yes	Classic	9,5	33	Negative	Negative	Negative	17	3	7
PD14288a	4	74	6,3	No	Classic	0,9	0	Positive	Positive	Negative	8	1	4
PD14289a	4	71	0,7	Yes	Solid	4,5	1	Positive	Positive	Negative	35	3	4
PD14290a	4	49	7	No	Alveolar	1,2	0	Positive	Positive	Negative	18	2	5
PD14291a	4	37	7,1	No	Classic	1,8		Positive	Negative	Negative	5	2	3
PD13891a	4	49	14,3	No	Classic	1,8		Positive	Negative	Negative	5	1	6
PD14292a	4	55	2,6	Yes	Alveolar	2,6	16	Positive	Positive	Positive	22	3	2
PD14293a	4	69	5,2	No	Alveolar	2	0	Positive	Positive	Negative	11	2	4
PD14294a	4	59	4,6	Yes	Solid	1,5	10	Positive	Negative	Negative	11	1	25
PD14295a	4	64	6,4	No	Mixed, non classic	2,5	0	Positive	Positive	Negative	23	3	1
PD14296a	4	62	7,4	No	Trabecular	3,3	1	Positive	Positive	Negative	3	2	2
PD13892a	4	43	9,8	Yes	Classic	6,3	2	Positive	Positive	Negative	30	3	12
PD14298a	4	55	5,9	No	Classic	4,5	0	Positive	Negative	Negative	8	2	6
PD14299a	4	47	7,5	No	Classic	2,3	0	Positive	Positive	Negative	12	2	4
PD14300a	4	49	5,5	No	Trabecular	4,5	1	Positive	Positive	Negative	15	2	5
PD14301a	4	44	7,3	No	Mixed, non classic	1,1	0	Positive	Positive	Negative	13	2	6
PD14302a	4	54	3,1	Yes	Mixed, non classic	3,5	27	Negative	Negative	Negative	48	3	30
PD14303a	4	64	1,5	Yes	Mixed, non classic	2,5	6	Positive	Negative	Positive	18	3	9
PD14304a	4	47	5,4	No	Solid	2,4	1	Positive	Positive	Negative	19	2	5
PD14305a	4	73	7,3	Yes	Trabecular	3	0	Positive	Negative	Negative	11	2	10
PD14306a	4	67	7,4	No	Mixed, non classic	1	0	Positive	Positive	Negative	15	2	20
PD14307a	4	66	3,6	Yes	Mixed, non classic	1,7	19	Negative	Negative	Negative	35	3	45
PD13893a	4	53	13,3	No	Mixed, non classic	2,5	29	Positive	Negative	Negative	22	2	9
PD14308a	4	39	5,7	No	Mixed, non classic	2,3	0	Positive	Positive	Negative	21	2	3
PD14309a	4	48	5,3	No	Trabecular	6,5	8	Positive	Positive	Negative	7	2	16
PD14310a	4	72	7,8	No	Mixed, non classic	2,5	1	Positive	Positive	Negative	18	2	1
PD14311a	4	63	4,9	No	Trabecular	1,5	1	Positive	Positive	Negative	25	2	2
PD14312a	4	55	7,2	No	Mixed, non classic	1,5	0	Positive	Positive	Negative	18	2	1
PD14313a	4	64	1,7	Yes	Solid	1	1	Positive	Positive	Positive	48	3	15
PD14314a	4	44	6,1	No	Trabecular	1,2	0	Positive	Positive	Positive	18	2	4
PD14316a	4	68	5,4	No	Classic	1,7	0	Positive	Positive	Negative	9	2	1
PD14317a	4	51	6,3	No	Trabecular	1,9	0	Positive	Positive	Negative	18	2	4
PD13894a	4	56	9,1	No	Classic	9	0	Positive	Positive	Negative	17	2	5
PD14319a	4	48	5,7	No	Classic	2,8	0	Positive	Negative	Negative	14	2	3
PD14320a	4	67	6	No	Classic	1,8	0	Positive	Positive	Negative	15	2	5
PD14321a	4	41	7,1	No	Trabecular	1,6	3	Positive	Positive	Negative	18	1	3

<u>Supplementary Table 3</u>: Patient and sample characteristics from the ER-positive/HER2-negative IDC and ILC tumors with TIL data from the BIG 2-98 study

	IDC (n=807)	**ILC (n=149)**	***P****
Age			
<50 years	427 (52.9)	54 (36.2)	<.001
≥50 years	380 (47.1)	95 (63.8)	
Grade			
Grade 1	84 (10.5)	12 (9.8)	<.001
Grade 2	428 (53.5)	88 (72.1)	
Grade 3	288 (36.0)	22 (18.0)	
Unknown	7	27	
Tumor size			
<2 cm	271 (33.7)	28 (18.9)	<.001
≥2 cm	533 (66.3)	120 (81.1)	
Unknown	3	1	
Positive lymph nodes			
1-3	461 (57.1)	69 (46.3)	.04
4-9	241 (29.9)	53 (35.6)	
>9	105 (13.0)	27 (18.1)	
PgR status			
Negative	77 (9.7)	9 (6.1)	.22
Positive	719 (90.3)	138 (93.9)	
Unknown	11	2	
Ki67 status			
<20%	386 (57.4)	99 (78.9)	<.001
≥20%	287 (42.6)	28 (22.0)	
Unknown	134	22	
Stromal TIL			
≤5%	159 (19.7)	41 (27.5)	.005
>5% and ≤10%	354 (43.9)	73 (49.0)	
>10%	294 (36.4)	35 (23.5)	

* Chi square test, two-sided.

<u>Supplementary Table 4</u>: Patient and sample characteristics from the ER-positive/HER2-negative IDC and ILC tumors from all cohorts considered in this manuscript

	Retrospective ILC cohort	BIG 2-98 ILC	BIG 2-98 IDC	Nottingham ILC	Notthingham IDC	CIBERSORT ILC	CIBERSORT IDC
Nr patients	614	149	807	159	468	296	1501
Age							
<50 years	201 (32.7)	54 (36.2)	427 (52.9)	34 (21.4)	155 (33.1)	47 (16.0)	284 (19.0)
≥50 years	413 (67.3)	95 (63.8)	380 (47.1)	125 (78.6)	313 (66.9)	247 (84.0)	1210 (81.0)
Unknown	0	0	0	0	0	2	7
Tumor size							
<2 cm	248 (40.4)	28 (18.9)	271 (33.7)	73 (45.9)	241 (51.6)	56 (19.1)	484 (32.4)
≥2 cm	366 (59.6)	120 (81.1)	533 (66.3)	86 (54.1)	226 (48.4)	237 (80.9)	1009 (67.6)
Unknown	0	1	3	0	1	3	8
Nodal status							
Negative	296 (50.0)	0 (0.0)	0 (0.0)	95 (65.1)	245 (58.2)	142 (48.3)	747 (50.0)
Positive	296 (50.0)	149 (100.0)	807 (100.0)	51 (34.9)	176 (41.8)	152 (51.7)	747 (50.0)
Unknown	22	0	0	13	47	2	7
Grade							
1	76 (12.5)	12 (9.8)	84 (10.5)	10 (6.3)	30 (6.4)	35 (13.7)	141 (9.6)
2	438 (71.9)	88 (72.1)	428 (53.5)	135 (84.9)	179 (38.3)	181 (71.0)	721 (49.3)
3	95 (15.6)	22 (18.0)	288 (36.0)	14 (8.8)	258 (55.2)	39 (15.3)	600 (41.1)
Unknown	5	27	7	0	1	41	39
Adj. Chemotherapy							
No	335 (54.7)	0 (0.0)	0 (0.0)	NA	NA	NA	NA
Yes	277 (45.3)	149 (100.0)	807 (100.0)	NA	NA	NA	NA
Unknown	2	0	0	NA	NA	NA	NA
Adj. Endocrine therapy							
No	63 (10.3)	9 (6.0)	46 (5.7)	NA	NA	NA	NA
Yes	551 (89.7)	140 (94.0)	761 (94.3)	NA	NA	NA	NA
Unknown	0	0	0	NA	NA	NA	NA

IDC : invasive ductal carcinoma, ILC: invasive lobular carcinoma.

<u>Supplementary Table 5</u>: Association between TIL and clinico-pathological variables in all ILC (n=614)

	Univariable model			Multivariable model		
	TIL % fold-change	**95%CI**	***P****	**TIL % fold-change**	**95%CI**	***P****
Age: ≥50y vs <50y	0.84	0.74 – 0.96	.01	0.85	0.74 – 0.98	.03
Size: ≥2cm vs <2cm	1.06	0.93 – 1.20	.39	1.01	0.88 – 1.15	.93
Grade: 3 vs 1-2	1.29	1.08 – 1.53	.005	1.04	0.85 – 1.28	.71
Histologic subtype:						
alveolar vs classic	0.81	0.68 – 0.97	.02	0.85	0.71 – 1.03	.10
mixed NC vs classic	1.39	1.16 – 1.67	<.001	1.25	1.02 – 1.53	.03
solid vs classic	1.03	0.86 – 1.24	.73	0.95	0.77 – 1.16	.60
trabecular vs classic	1.12	0.85 – 1.49	.42	1.04	0.78 – 1.38	.81
			<.001°			.03°
Nodal status: + vs -	1.21	1.07 – 1.38	.003	1.13	0.99 – 1.29	.07
Ki67: + vs -	1.25	1.09 – 1.43	.001	1.17	1.00 – 1.37	.04
ER: + vs -	0.56	0.43 – 0.73	<.001	0.70	0.52 – 0.93	.02
PgR: + vs -	0.84	0.73 – 0.98	.02	0.86	0.73 – 1.01	.07
HER2: + vs -	1.31	0.97 – 1.78	.08	1.06	0.78 – 1.44	.72

* The two-sided *P*-values were calculated using univariable and multiple linear regression models of log-transformed TIL percentage versus clinico-pathological variables.

° The two-sided P-values were calculated using a F-test.

CI: confidence interval, ER: estrogen receptor, ILC: invasive lobular carcinoma, PgR: progesterone receptor; TIL: tumor infiltrating lymphocyte.

<u>Supplementary Table 6:</u> Association between TIL and clinico-pathological variables in ILC patients from BIG 2-98 (n=204)

	Univariable model			Multivariable model		
	TIL % fold-change	**95%CI**	***P****	**TIL % fold-change**	**95%CI**	***P****
Age: ≥50y vs <50y	0.77	0.64 – 0.92	.005	0.75	0.60 – 0.95	.02
Size: ≥2cm vs <2cm	1.07	0.85 – 1-34	.57	1.05	0.80 – 1.39	.72
Grade: 3 vs 1-2	1.15	0.88 – 1.48	.31	0.97	0.74 – 1.29	.85
Positive nodes: >3 vs 1-3	0.98	0.81 – 1.17	.81	0.97	0.77 – 1.21	.78
Ki67: ≥20% vs <20%	1.36	1.08 – 1.71	.009	1.32	1.02 – 1.71	.04
ER: + vs -	0.92	0.65 – 1.30	.62	0.87	0.38 – 2.00	.75
PgR: + vs -	0.82	0.63 – 1.07	.14	0.78	0.48 – 1.26	.31
HER2: + vs -	1.34	0.88 – 2.04	.17	1.36	0.82 – 2.27	.23

* The two-sided *P*-values were calculated using univariable and multiple linear regression models of log-transformed TIL percentage versus clinico-pathological variables.

CI: confidence interval, ER: estrogen receptor, ILC: invasive lobular carcinoma, PgR: progesterone receptor; TIL: tumor infiltrating lymphocyte.

<u>Supplementary Table 7</u>: Association between TIL and clinico-pathological variables in ER-positive/HER2-negative ILC (n=555)

	Univariable model			Multivariable model		
	TIL % fold-change	**95%CI**	***P****	**TIL % fold-change**	**95%CI**	***P****
Age: ≥50y vs <50y	0.81	0.71 – 0.93	.003	0.83	0.72 – 0.96	.01
Size: ≥2cm vs <2cm	1.1	0.97 – 1.26	.14	1.09	0.94 – 1.25	.25
Grade: 3 vs 1-2	1.04	0.85 – 1.27	.68	0.94	0.75 – 1.17	.56
Histologic subtype:						
alveolar vs classic	0.8	0.67 – 0.95	.01	0.84	0.70 – 1.02	.08
mixed NC vs classic	1.22	1.00 – 1.48	.05	1.15	0.94 – 1.42	.17
solid vs classic	1.01	0.83 – 1.23	.91	0.98	0.80 – 1.21	.87
trabecular vs classic	1.14	0.86 – 1.52	.35	1.05	0.79 – 1.41	.72
			.006°			.14°
Nodal status: + vs -	1.15	1.01 – 1.31	.04	1.08	0.95 – 1.24	.25
Ki67: + vs -	1.16	1.01 – 1.34	.04	1.16	0.99 – 1.35	.07
PgR: + vs -	1.00	0.85 – 1.18	.99	0.94	0.79 – 1.12	.49

* The two-sided *P*-values were calculated using univariable and multiple linear regression models of log-transformed TIL percentage versus clinico-pathological variables.

° The two-sided P-values were calculated using a two-sided F-test.

CI: confidence interval, ER: estrogen receptor, ILC: invasive lobular carcinoma, PgR: progesterone receptor; TIL: tumor infiltrating lymphocyte

<u>Supplementary Table 8</u>: Association between TIL and clinico-pathological variables in ER-positive/HER2-negative ILC patients from BIG 2-98 (n=149)

	Univariable model			Multivariable model		
	TIL % fold-change	**95%CI**	***P****	**TIL % fold-change**	**95%CI**	***P****
Age: ≥50y vs <50y	0.75	0.61 – 0.91	.005	0.77	0.61 – 0.97	.03
Size: ≥2cm vs <2cm	1.01	0.78 – 1.30	.97	1.12	0.84 – 1.48	.45
Grade: 3 vs 1-2	0.97	0.74 – 1.28	.83	0.93	0.69 – 1.24	.62
Positive nodes: >3 vs 1-3	0.91	0.74 – 1.10	.33	0.96	0.77 – 1.21	.75
Ki67: ≥20% vs <20%	1.38	1.07 – 1.78	.01	1.43	1.10 – 1.86	.01
PgR: + vs -	0.74	0.49 – 1.12	.16	0.81	0.48 – 1.37	.44

* The two-sided *P*-values were calculated using univariable and multiple linear regression models of log-transformed TIL percentage versus clinico-pathological variables.

CI: confidence interval, ER: estrogen receptor, ILC: invasive lobular carcinoma, PgR: progesterone receptor; TIL: tumor infiltrating lymphocyte

<u>Supplementary Table 9</u>: Association between TIL and clinico-pathological variables in ER-positive/HER2-negative IDC patients from BIG 2-98 (n=807)

	Univariable model			Multivariable model		
	TIL % fold-change	**95%CI**	***P****	**TIL % fold-change**	**95%CI**	***P****
Age: ≥50y vs <50y	0.99	0.90 – 1.08	0.79	1.06	0.96 – 1.17	.22
Size: ≥2cm vs <2cm	1.05	0.95 – 1.15	0.35	1.00	0.90 – 1.11	.97
Grade: 3 vs 1-2	1.25	1.14 – 1.37	<.001	1.13	1.01 – 1.25	.03
Positive nodes: >3 vs 1-3	1.09	0.99 – 1.19	0.07	1.04	0.94 – 1.15	.47
Ki67: ≥20% vs <20%	1.26	1.14 – 1.39	<.001	1.21	1.09 – 1.34	<.001
PgR: + vs -	0.9	0.77 – 1.06	0.20	0.92	0.78 – 1.09	.35

* The two-sided *P*-values were calculated using univariable and multiple linear regression models of log-transformed TIL percentage versus clinico-pathological variables.

CI: confidence interval, ER: estrogen receptor, IDC: invasive ductal carcinoma, PgR: progesterone receptor; TIL: tumor infiltrating lymphocyte.

<u>Supplementary Table 10</u>: Association between TIL and recurrently mutated genes in ILC

	Unadjusted model			Adjusted model*		
	TILs % fold-change	**95%CI**	***P*†**	**TILs % fold-change**	**95%CI**	***P*†**
AKT1	0.91	0.62 – 1.34	.64	0.95	0.65 – 1.38	.78
ARID1A	1.39	1.02 – 1.91	.04	1.41	1.02 – 1.96	.04
BRCA2	1.71	1.01 – 2.87	.04	1.6	0.97 – 2.66	.07
CDH1	1.00	0.85 – 1.18	.99	1.01	0.86 – 1.18	.93
ERBB2	1.02	0.72 – 1.44	.93	0.87	0.60 – 1.25	.45
ERBB3	0.54	0.36 – 0.82	.004	0.56	0.37 – 0.85	.006
FOXA1	1.04	0.79 – 1.37	.76	1.06	0.80 – 1.40	.68
GATA3	1.01	0.75 – 1.36	.93	1.08	0.80 – 1.44	.63
MAP3K1	1.12	0.80 – 1.58	.51	1.18	0.84 – 1.64	.34
KMT2C	1.27	0.96 – 1.69	.10	1.32	0.99 – 1.76	.06
PIK3CA	1.10	0.94 – 1.29	.23	1.1	0.94 – 1.29	.24
PTEN	0.95	0.63 – 1.43	.81	0.89	0.59 – 1.32	.56
RUNX1	0.97	0.64 – 1.48	.89	0.85	0.55 – 1.30	.46
TBX3	1.08	0.86 – 1.36	.52	1.11	0.88 – 1.40	.39
TP53	1.51	1.13 – 2.02	.006	1.45	1.07 – 1.96	.02

†The two-sided *P*-values were calculated using univariable and multiple linear regression models of log-transformed TIL percentage versus genomic alterations.

***** Model adjusted for age, tumor size, tumor grade, nodal status, histological subtype, and Ki67, ER, PgR and HER2 status.

CI: confidence interval, ER: estrogen receptor, ILC: invasive lobular carcinoma, PgR: progesterone receptor; TIL: tumor infiltrating lymphocyte.

Supplementary Table 11: Association between TIL and recurrent CNAs in ILC

	Unadjusted model			Adjusted model*		
	TILs % fold-change	**95%CI**	***P*†**	**TILs % fold-change**	**95%CI**	***P*†**
chr1_p_loss	0.86	0.53 – 1.39	.54	0.78	0.46 – 1.33	.37
chr4_p_loss	1.08	0.74 – 1.57	.68	0.89	0.61 – 1.30	.54
chr5_p_gain	0.94	0.62 – 1.41	.77	0.94	0.62 – 1.42	.76
chr7_p_gain	0.87	0.54 – 1.40	.57	0.82	0.51 – 1.32	.41
chr8_p_gain	0.99	0.64 – 1.54	.97	0.92	0.59 – 1.43	.71
chr8_p_loss	1.26	0.87 – 1.83	.22	0.98	0.66 – 1.48	.94
chr9_p_loss	0.85	0.54 – 1.34	.49	1.11	0.68 – 1.81	.68
chr11_p_gain	0.87	0.54 – 1.41	.58	0.97	0.59 – 1.61	.91
chr16_p_gain	0.99	0.78 – 1.27	.96	1.02	0.79 – 1.30	.89
chr17_p_loss	1.07	0.85 – 1.36	.55	1.06	0.85 – 1.34	.60
chr18_p_gain	1.29	0.82 – 2.04	.27	1.24	0.79 – 1.95	.36
chr18_p_loss	0.88	0.66 – 1.19	.42	0.90	0.66 – 1.23	.50
chr20_p_gain	0.96	0.61 – 1.52	.86	0.95	0.59 – 1.51	.82
chr1_q_gain	0.8	0.63 – 1.02	.08	0.81	0.63 – 1.04	.10
chr5_q_gain	0.65	0.43 – 0.98	.04	0.68	0.45 – 1.02	.07
chr6_q_loss	0.70	0.46 – 1.07	.10	0.71	0.47 – 1.06	.10
chr8_q_gain	0.79	0.56 – 1.13	.21	0.77	0.54 – 1.10	.15
chr13_q_loss	0.96	0.66 – 1.40	.85	1.07	0.72 – 1.58	.74
chr15_q_loss	1.37	0.85 – 2.20	.20	1.28	0.79 – 2.07	.31
chr16_q_loss	0.84	0.58 – 1.21	.35	1.02	0.69 – 1.49	.93
chr17_q_loss	0.87	0.56 – 1.35	.53	0.88	0.57 – 1.37	.58
chr18_q_loss	1.02	0.74 – 1.40	.89	1.04	0.75 – 1.45	.81
chr20_q_gain	0.71	0.45 – 1.11	.13	0.74	0.48 – 1.16	.19
chr21_q_gain	0.78	0.54 – 1.12	.18	0.80	0.55 – 1.17	.25
chr22_q_loss	0.96	0.75 – 1.23	.77	0.98	0.76 – 1.26	.86
chr6q25_1_gain	0.96	0.74 – 1.24	.75	1.03	0.79 – 1.34	.85
chr7p21_2_gain	1.28	1.03 – 1.61	.03	1.34	1.07 – 1.67	.01
chr8p11_23_gain	0.89	0.69 – 1.16	.39	0.84	0.64 – 1.09	.19
chr8q24_21_gain	1.04	0.82 – 1.33	.75	0.98	0.77 – 1.25	.87
chr11q13_3_gain	0.91	0.72 – 1.15	.42	0.92	0.71 – 1.19	.54
chr11q14_1_gain	0.79	0.61 – 1.01	.06	0.79	0.60 – 1.04	.09
chr12q24_21_gain	0.92	0.69 – 1.23	.59	0.90	0.67 – 1.19	.46
chr15q26_3_gain	0.91	0.71 – 1.16	.46	0.99	0.78 – 1.26	.92
chr17q12_gain	1.12	0.85 – 1.47	.41	1.06	0.78 – 1.45	.71
chr17q23_1_gain	1.02	0.75 – 1.38	.91	0.98	0.71 – 1.34	.88
chr1p36_22_loss	1.05	0.81 – 1.38	.70	0.96	0.70 – 1.30	.77
chr2p23_2_loss	1.30	0.98 – 1.72	.07	1.10	0.83 – 1.48	.50
chr3p21_31_loss	1.34	0.96 – 1.86	.09	1.35	0.96 – 1.90	.08
chr6q21_loss	0.82	0.65 – 1.05	.11	0.83	0.65 – 1.06	.14
chr7p22_2_loss	1.25	0.94 – 1.66	.13	1.25	0.95 – 1.65	.11
chr8p22_loss	0.97	0.75 – 1.24	.78	0.91	0.70 – 1.17	.45
chr8q24_23_loss	1.50	1.11 – 2.02	.008	1.66	1.22 – 2.26	.002
chr11q11_loss	1.06	0.82 – 1.38	.63	1.10	0.85 – 1.42	.48
chr11q23_1_loss	0.92	0.73 – 1.15	.47	0.96	0.76 – 1.22	.73
chr12q24_32_loss	1.00	0.77 – 1.30	1.00	1.02	0.78 – 1.32	.90

†The two-sided *P*-values were calculated using univariable and multiple linear regression models of log-transformed TIL percentage versus genomic alterations.

***** Model adjusted for age, tumor size, tumor grade, nodal status, histological subtype, and Ki67, ER, PgR and HER2 status.

CNA: copy number aberration, CI: confidence interval, ER: estrogen receptor, ILC: invasive lobular carcinoma, PgR: progesterone receptor; TIL: tumor infiltrating lymphocyte.

<u>Supplementary Table 12</u>: Univariable and multivariable Cox proportional hazard analyses with TIL as a continuous variable in all ILC from the retrospective series

	Univariable model			**Multivariable model**†		
	HR	**95%CI**	***P****	**HR**	**95%CI**	***P****
Continuous TIL (10% units)	1.22	1.06 – 1.41	.005	1.06	0.90 – 1.26	.49
Age (≥50 vs <50 yrs)	1.36	0.96 – 1.92	.08	1.41	0.98 – 2.03	.07
Size (≥ 2 vs <2 cm)	2.09	1.47 – 2.98	<0.001	1.68	1.14– 2.46	.008
Grade (3 vs 1-2)	2.31	1.62 – 3.29	<.001	1.42	0.91 – 2.21	.12
Nodal status (+ vs -)	3.25	2.26 – 4.67	<.001	2.87	1.87 – 4.39	<.001
Ki67 (+ vs -)	2.21	1.61 – 3.03	<.001	1.75	1.21 – 2.54	.003
ER (+ vs -)	0.39	0.24 – 0.64	<.001	0.69	0.34 – 1.40	.30
PgR (+ vs -)	0.72	0.50 – 1.02	.06	0.80	0.53 – 1.22	.30
HER2 (+ vs -)	2.60	1.47 – 4.58	.001	1.50	0.81 – 2.80	.20
Adj. chemotherapy (yes vs no)	1.80	1.31 – 2.48	<.001	0.94	0.63 – 1.40	.75
Adj. endocrine therapy (yes vs no)	0.58	0.37 – 0.91	.02	1.02	0.52 – 1.97	.96

***** The two-sided *P*-values were issued from the Cox regression analysis.

†Cox regression model including categorical TIL, age, tumor size, tumor grade, nodal status, Ki67, ER, PgR and HER2 status, adjuvant chemotherapy and adjuvant endocrine therapy.

CI: confidence interval, ER: estrogen receptor, ILC: invasive lobular carcinoma, PgR: progesterone receptor; TIL: tumor infiltrating lymphocyte.

<u>Supplementary Table 13</u>: Univariable and multivariable Cox proportional hazard analyses with TIL as a categorical variable in all ILC from the retrospective series

	Univariable model			Multivariable model†		
	HR	**95%CI**	***P****	**HR**	**95%CI**	***P****
TILs						
intermediate vs low	1.46	1.02 – 2.09	.04	1.55	1.06 – 2.27	.02
high vs low	1.84	1.22 – 2.78	.004	1.26	0.79 – 1.99	.33
			.008°			0.08°
Age (≥ 50 vs <50 yrs)	1.36	0.96 – 1.92	.08	1.45	1.00 – 2.10	.05
Size (≥ 2 vs < 2cm)	2.09	1.47 – 2.98	<.001	1.70	1.16 – 2.50	.007
Grade (3 vs 1-2)	2.31	1.62 – 3.29	<.001	1.48	0.95 – 2.30	.08
Nodal status (+ vs -)	3.25	2.26 – 4.67	<.001	2.92	1.90 – 4.47	<.001
Ki67 (+ vs -)	2.21	1.61 – 3.03	<.001	1.77	1.22 – 2.55	.002
ER (+ vs -)	0.39	0.24 – 0.64	<.001	0.66	0.32 – 1.34	.25
PgR (+ vs -)	0.72	0.50 – 1.02	.06	0.80	0.52 – 1.22	.30
HER2 (+ vs -)	2.60	1.47 – 4.58	.001	1.49	0.79 – 2.81	.21
Adj. chemotherapy (yes vs no)	1.80	1.31 – 2.48	<.001	0.90	0.60 – 1.35	.61
Adj. endocrine therapy (yes vs no)	0.58	0.37 – 0.91	.02	1.06	0.55 – 2.08	.86

***** The two-sided *P*-values were issued from the Cox regression analysis.

†Cox regression model including categorical TIL, age, tumor size, tumor grade, nodal status, Ki67, ER, PgR and HER2 status, adjuvant chemotherapy and adjuvant endocrine therapy.

° The two-sided P-values were calculated using the global Wald test.

CI: confidence interval, ER: estrogen receptor, HR: hazard ratio, ILC: invasive lobular carcinoma, PgR: progesterone receptor; TIL: tumor infiltrating lymphocyte.

<u>Supplementary Table 14:</u> Univariable and multivariable Cox proportional hazard analyses with TIL as a categorical or continuous variable in the ER-positive/HER2-negative ILC from the retrospective series

	Univariable Cox model			Multivariable Cox model†		
	HR	**95% CI**	***P****	**HR**	**95% CI**	***P****
TIL%			.13°			.17°
5< ≤10 vs ≤5	1.30	0.88-1.92	.19	1.41	0.93-2.13	.10
>10 vs ≤5	1.58	0.98-2.54	.06	1.43	0.86-2.37	.17
TIL (10% units)	1.11	0.90-1.36	.32	1.04	0.85-1.28	.71

***** The two-sided *P*-values were issued from the Cox regression analysis.

†Cox regression model including categorical TIL, age (<50y or ≥50y), grade (G1-2 or G3), size (<2cm or ≥2cm), lymph nodes (0 or >0), Ki67 (<20 or ≥20), PgR (negative or positive), adjuvant chemotherapy (no or yes) and adjuvant endocrine therapy (no or yes).

° The two-sided P-values were calculated using the global Wald test.

CI: confidence interval, ER: estrogen receptor, HR: hazard ratio, ILC: invasive lobular carcinoma, PgR: progesterone receptor; TIL: tumor infiltrating lymphocyte.

<u>Supplementary Table 15</u>: Univariable Cox proportional hazard analyses with TIL as a categorical and continuous variable in the ER-negative and/or HER2-positive ILC from the retrospective series

	Univariable Cox model		
	HR	95% CI	*P**
TIL%			.35°
5< ≤10 vs ≤5	1.93	0.73-5.07	.18
>10 vs ≤5	1.84	0.70-4.83	.22
TIL (10% units)	1.32	1.01-1.74	.04

***** The two-sided *P*-values were issued from the Cox regression analysis.

° The two-sided P-values were calculated using the global Wald test.

CI: confidence interval, ER: estrogen receptor, HR: hazard ratio, ILC: invasive lobular carcinoma, PgR: progesterone receptor; TIL: tumor infiltrating lymphocyte.

<u>Supplementary Table 16</u>: Univariable and multivariable Cox proportional hazard analyses with TIL as a categorical and continuous variable in all ILC from the BIG 2-98 series

	Univariable Cox model			**Multivariable Cox model†**		
	HR	95% CI	*P**	HR	95% CI	*P**
TIL%			.24°			.88°
5< ≤10 vs ≤5	1.43	0.83-2.48	.20	1.06	0.44-2.56	.90
>10 vs ≤5	1.68	0.90-3.13	.10	1.26	0.46-3.46	.65
TIL (10% units)	1.06	0.82-1.37	.64	1.09	0.68-1.76	.72

***** The two-sided *P*-values were issued from the Cox regression analysis.

†Cox regression model including categorical TIL, age (<50y or ≥50y), grade (G1, G2 or G3), size (<2cm or ≥2cm), lymph nodes (1-3 4-9 or >9), Ki67 (<10, 10≤ <20 or ≥20) and PgR (negative or positive).

° The two-sided P-values were calculated using the global Wald test on categorical TIL.

CI: confidence interval, ER: estrogen receptor, HR: hazard ratio, ILC: invasive lobular carcinoma, PgR: progesterone receptor; TIL: tumor infiltrating lymphocyte.

<u>Supplementary Table 17</u>: Univariable and multivariable Cox proportional hazard analyses with TIL as a categorical and continuous variable in the ER-positive/HER2-negative ILC from the BIG 2-98 series

	Univariable Cox model			**Multivariable Cox model†**		
	HR	95% CI	*P**	HR	95% CI	*P**
TIL%			.29°			..69°
5< ≤10 vs ≤5	1.49	0.74-2.98	.26	0.95	0.39-2.33	.91
>10 vs ≤5	1.85	0.86-3.99	.12	1.36	0.47-3.98	.57
TIL (10% units)	1.07	0.80-1.41	.66	1.32	0.75-4.43	.35

***** The two-sided *P*-values were issued from the Cox regression analysis.

†Cox regression model including categorical TIL, age (<50y or ≥50y), grade (G1, G2 or G3), size (<2cm or ≥2cm), lymph nodes (1-3 4-9 or >9), Ki67 (<10, 10≤ <20 or ≥20) and PgR (negative or positive).

° The two-sided P-values were calculated using the global Wald test on categorical TIL.

CI: confidence interval, ER: estrogen receptor, HR: hazard ratio, ILC: invasive lobular carcinoma, PgR: progesterone receptor; TIL: tumor infiltrating lymphocyte.

<u>Supplementary Table 18</u>: Univariable and multivariable Cox proportional hazard analyses with TIL as a categorical and continuous variable in the ER-positive/HER2-negative IDC from the BIG 2-98 series

	Univariable Cox model			**Multivariable Cox model†**		
	HR	95% CI	*P**	HR	95% CI	*P**
TIL%			.40°			.74°
5< ≤10 vs ≤5	0.80	0.58-1.11	.19	0.90	0.60-1.34	.61
>10 vs ≤5	0.90	0.65-1.26	.55	0.85	0.57-1.28	.44
TIL (10% units)	1,07	0.96-1.20	.22	0.98	0.86-1.11	.71

***** The two-sided *P*-values were issued from the Cox regression analysis.

†Cox regression model including categorical TIL, age (<50y or ≥50y), grade (G1, G2 or G3), size (<2cm or ≥2cm), lymph nodes (1-3 4-9 or >9), Ki67 (<10, 10≤ <20 or ≥20) and PgR (negative or positive).

° The two-sided P-values were calculated using the global Wald test on categorical TIL.

CI: confidence interval, ER: estrogen receptor, HR: hazard ratio, ILC: invasive lobular carcinoma, PgR: progesterone receptor; TIL: tumor infiltrating lymphocyte.

Figure 1

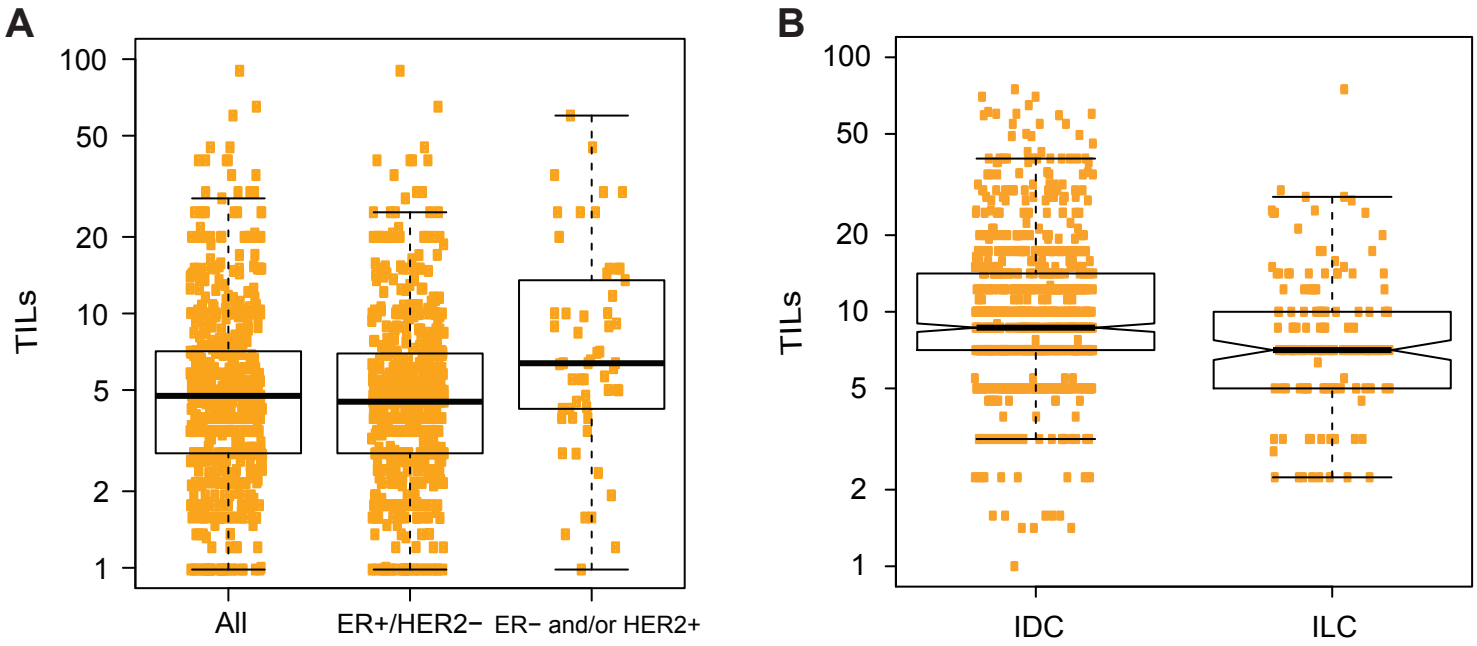
A
100
50
20
10
5
2
1
TILs
All
ER+/HER2−
ER− and/or HER2+
B
100
50
20
10
5
2
1
TILs
IDC
ILC

Figure 2

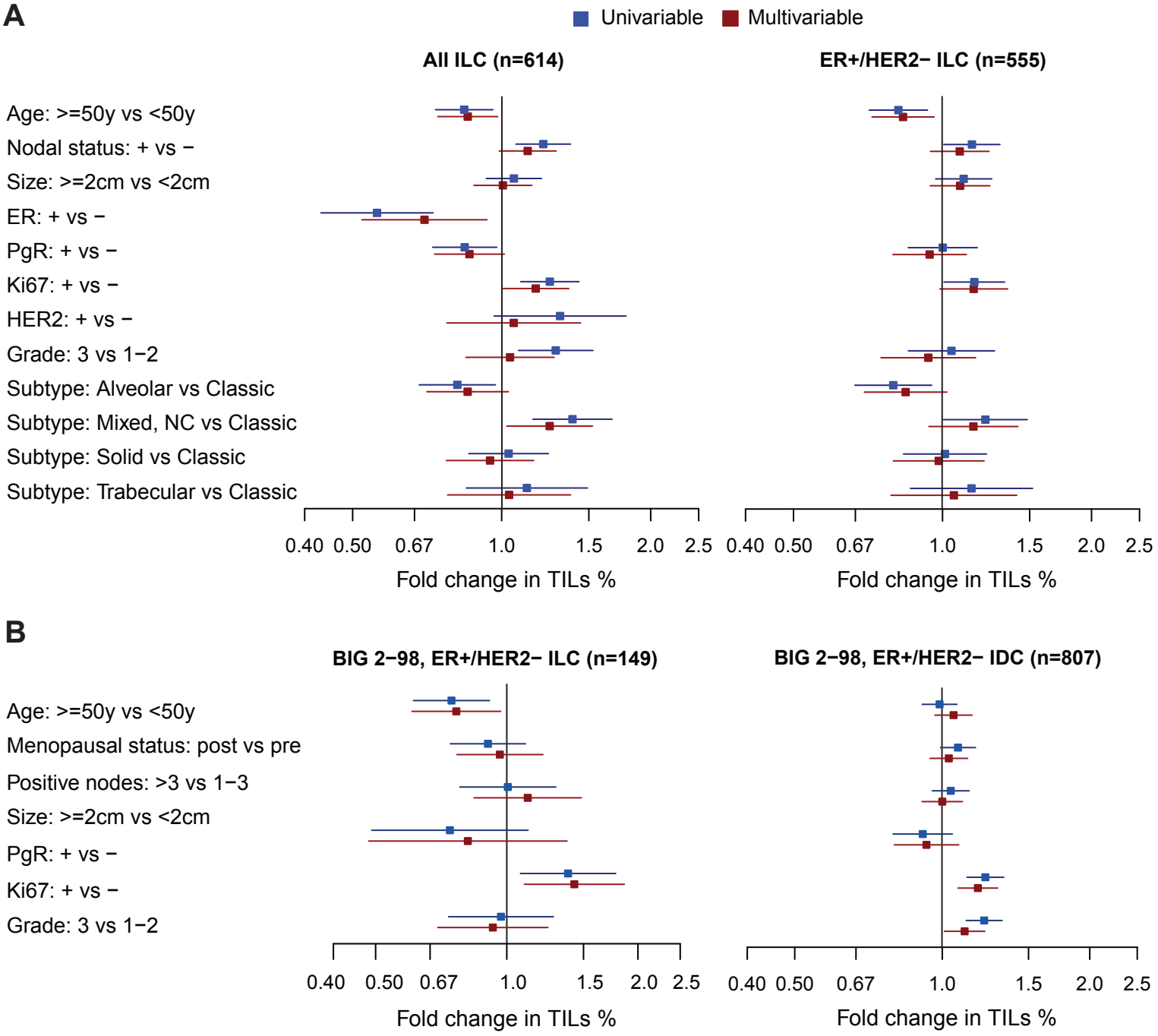
A
Univariable
Multivariable
All ILC (n=614)
ER+/HER2− ILC (n=555)
Age: >=50y vs <50y
Nodal status: + vs −
Size: >=2cm vs <2cm
ER: + vs −
PgR: + vs −
Ki67: + vs −
HER2: + vs −
Grade: 3 vs 1−2
Subtype: Alveolar vs Classic
Subtype: Mixed, NC vs Classic
Subtype: Solid vs Classic
Subtype: Trabecular vs Classic
0.40 0.50 0.67 1.0 1.5 2.0 2.5
Fold change in TILs %
B
BIG 2−98, ER+/HER2− ILC (n=149)
BIG 2−98, ER+/HER2− IDC (n=807)
Age: >=50y vs <50y
Menopausal status: post vs pre
Positive nodes: >3 vs 1−3
Size: >=2cm vs <2cm
PgR: + vs −
Ki67: + vs −
Grade: 3 vs 1−2
0.40 0.50 0.67 1.0 1.5 2.0 2.5
Fold change in TILs %

Figure 3

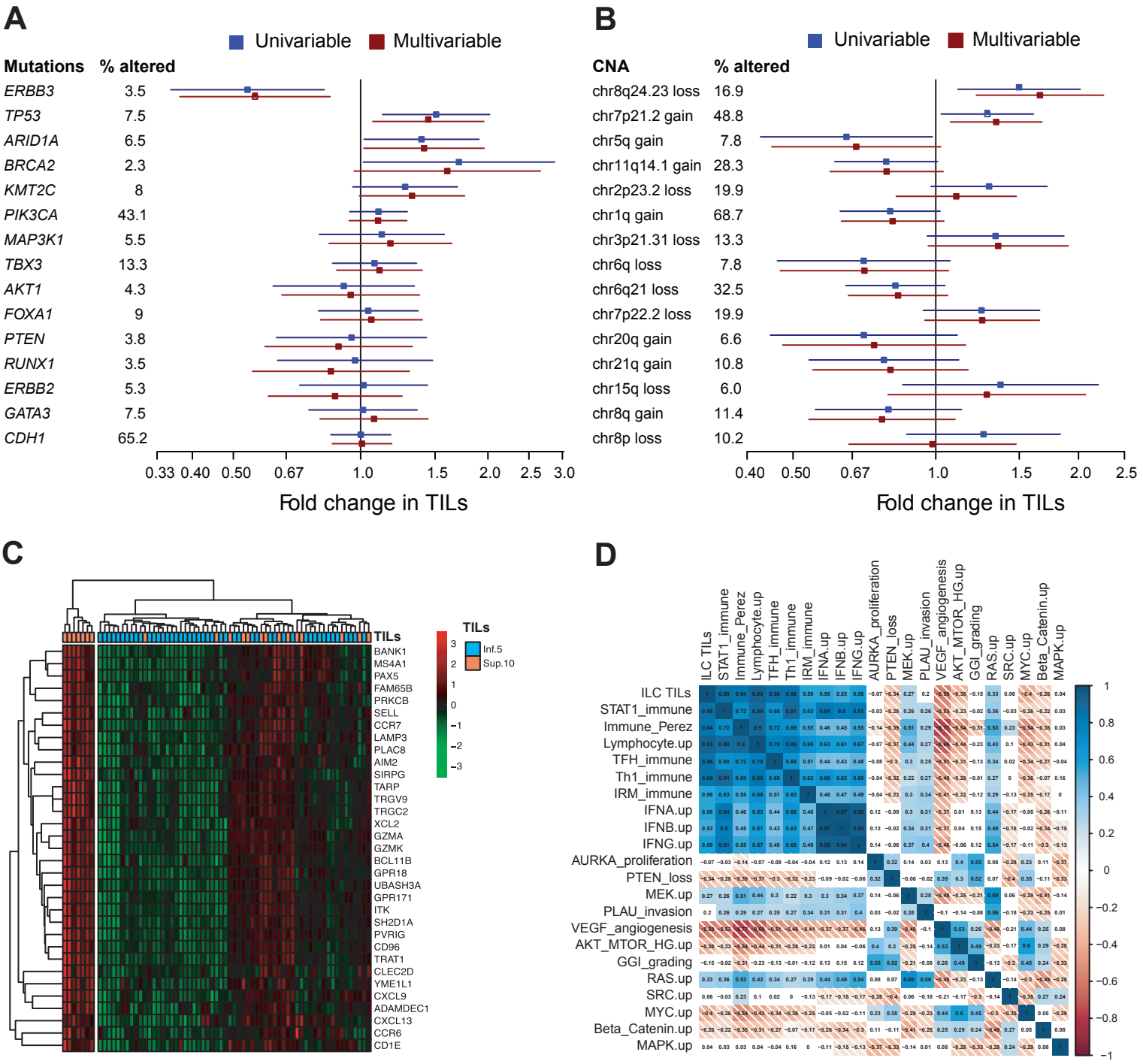
A
Univariable
Multivariable
Mutations
% altered
ERBB3 3.5
TP53 7.5
ARID1A 6.5
BRCA2 2.3
KMT2C 8
PIK3CA 43.1
MAP3K1 5.5
TBX3 13.3
AKT1 4.3
FOXA1 9
PTEN 3.8
RUNX1 3.5
ERBB2 5.3
GATA3 7.5
CDH1 65.2
0.33 0.40 0.50 0.67 1.0 1.5 2.0 2.5 3.0
Fold change in TILs
B
Univariable
Multivariable
CNA
% altered
chr8q24.23 loss 16.9
chr7p21.2 gain 48.8
chr5q gain 7.8
chr11q14.1 gain 28.3
chr2p23.2 loss 19.9
chr1q gain 68.7
chr3p21.31 loss 13.3
chr6q loss 7.8
chr6q21 loss 32.5
chr7p22.2 loss 19.9
chr20q gain 6.6
chr21q gain 10.8
chr15q loss 6.0
chr8q gain 11.4
chr8p loss 10.2
0.40 0.50 0.67 1.0 1.5 2.0 2.5
Fold change in TILs

C
TILs
Inf.5
Sup.10
3
2
1
0
−1
−2
−3
TILs
BANK1
MS4A1
PAX5
FAM65B
PRKCB
SELL
CCR7
LAMP3
PLAC8
AIM2
SIRPG
TARP
TRGV9
TRGC2
XCL2
GZMA
GZMK
BCL11B
GPR18
UBASH3A
GPR171
ITK
SH2D1A
PVRIG
CD96
TRAT1
CLEC2D
YME1L1
CXCL9
ADAMDEC1
CXCL13
CCR6
CD1E

D
ILC TILs
STAT1_immune
Immune_Perez
Lymphocyte.up
TFH_immune
Th1_immune
IRM_immune
IFNA.up
IFNB.up
IFNG.up
AURKA_proliferation
PTEN_loss
MEK.up
PLAU_invasion
VEGF_angiogenesis
AKT_MTOR_HG.up
GGI_grading
RAS.up
SRC.up
MYC.up
Beta_Catenin.up
MAPK.up
1
0.8
0.6
0.4
0.2
0
−0.2
−0.4
−0.6
−0.8
−1

Figure 4

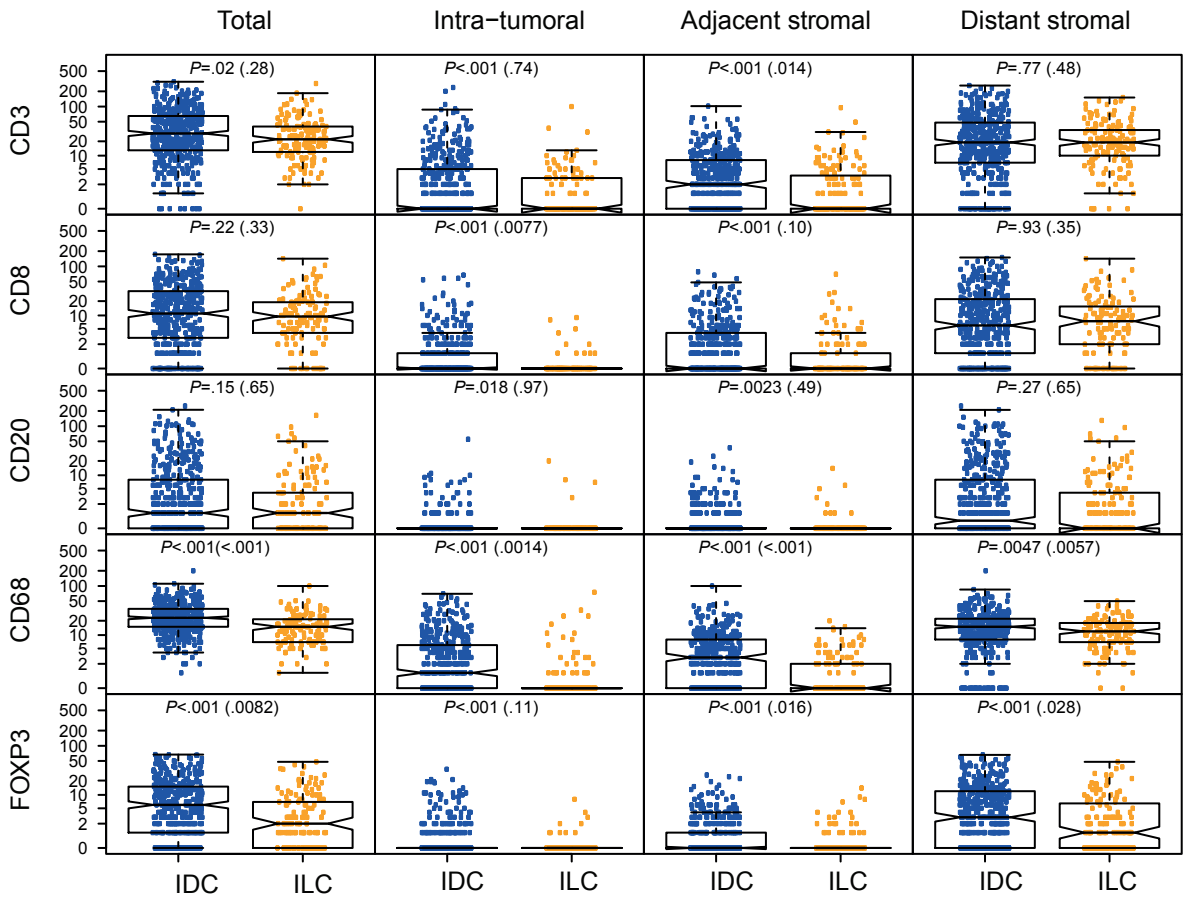
Total
Intra−tumoral
Adjacent stromal
Distant stromal
CD3
CD8
CD20
CD68
FOXP3
P=.02 (.28)
P<.001 (.74)
P<.001 (.014)
P=.77 (.48)
P=.22 (.33)
P<.001 (.0077)
P<.001 (.10)
P=.93 (.35)
P=.15 (.65)
P=.018 (.97)
P=.0023 (.49)
P=.27 (.65)
P<.001(<.001)
P<.001 (.0014)
P<.001 (<.001)
P=.0047 (.0057)
P<.001 (.0082)
P<.001 (.11)
P<.001 (.016)
P<.001 (.028)
500
200
100
50
20
10
5
2
0
IDC
ILC

Figure 5

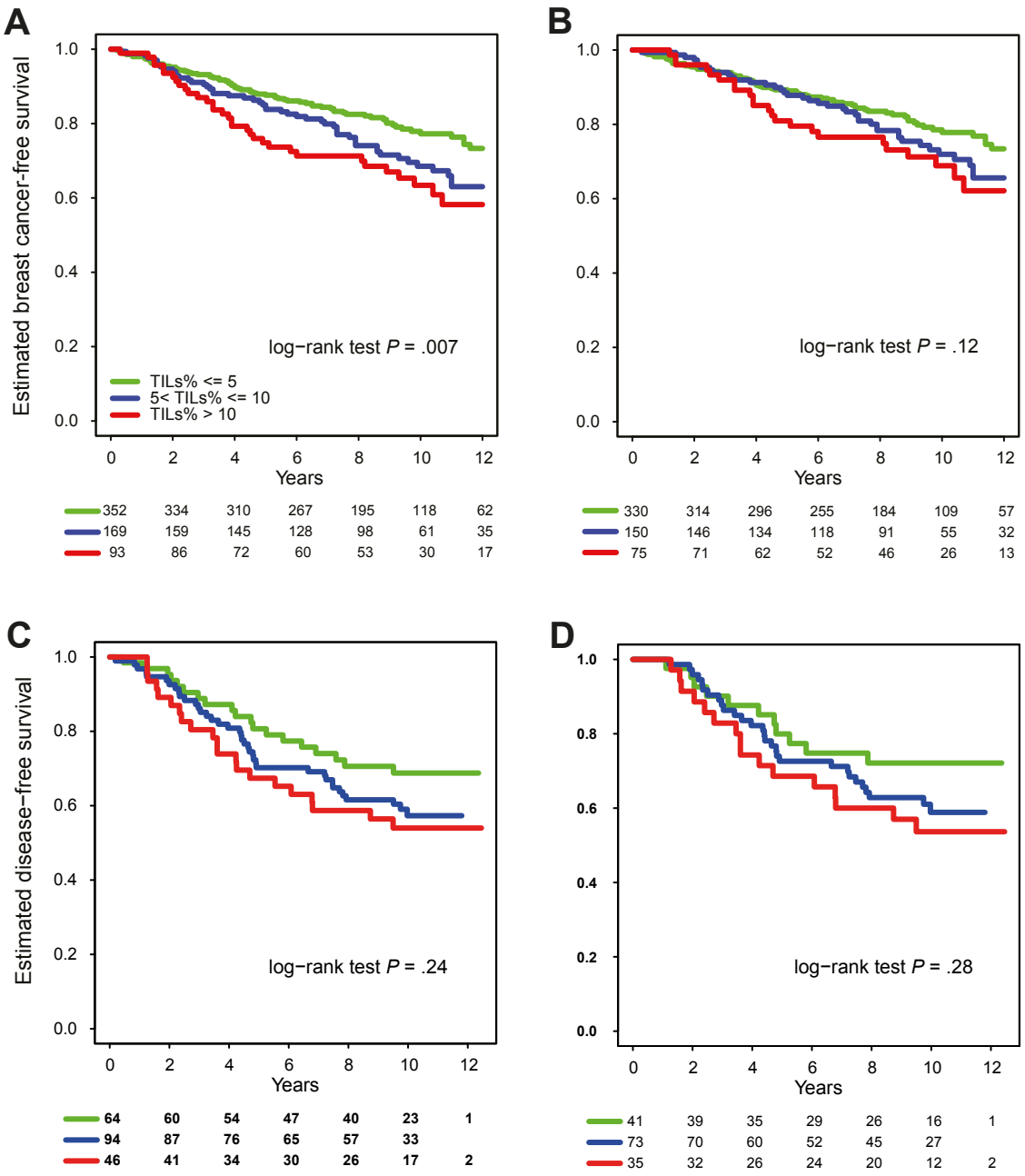
A
Estimated breast cancer-free survival
1.0
0.8
0.6
0.4
0.2
0.0
log−rank test P = .007
TILs% <= 5
5< TILs% <= 10
TILs% > 10
0 2 4 6 8 10 12
Years
352 334 310 267 195 118 62
169 159 145 128 98 61 35
93 86 72 60 53 30 17
B
log−rank test P = .12
Years
330 314 296 255 184 109 57
150 146 134 118 91 55 32
75 71 62 52 46 26 13
C
Estimated disease−free survival
log−rank test P = .24
Years
64 60 54 47 40 23 1
94 87 76 65 57 33
46 41 34 30 26 17 2
D
log−rank test P = .28
Years
41 39 35 29 26 16 1
73 70 60 52 45 27
35 32 26 24 20 12 2